INDICATORS OF INFLAMMATION IN THE FASTING INDUCED FATTY LIVER OF THE AMERICAN MINK (*NEOVISON VISON*)

by

Timothy D. Martin

Submitted in partial fulfilment of the requirements
for the degree of Master of Science

at

Dalhousie University
Halifax, Nova Scotia
November 2012

DALHOUSIE UNIVERSITY

FACULTY OF AGRICULTURE

The undersigned hereby certify that they have read and recommend to the Faculty of Graduate Studies for acceptance a thesis entitled "INDICATORS OF INFLAMMATION IN THE FASTING INDUCED FATTY LIVER OF THE AMERICAN MINK (*NEOVISON VISON*)" by Timothy D. Martin in partial fulfilment of the requirements for the degree of Master of Science.

Dated: November 26, 2012

Supervisor: _____

Readers: _____

_____

_____

DALHOUSIE UNIVERSITY

DATE: November 26, 2012

AUTHOR: Timothy D. Martin

TITLE: INDICATORS OF INFLAMMATION IN THE FASTING INDUCED FATTY LIVER OF THE AMERICAN MINK (*NEOVISON VISON*)

DEPARTMENT OR SCHOOL: Faculty of Agriculture

DEGREE: MSc CONVOCATION: May YEAR: 2013

_____

Signature of Author

TABLE OF CONTENTS

LIST OF TABLES

LIST OF FIGURES

ABSTRACT

The presence of inflammation in the progression of fatty liver disease induced by fasting was determined in mink. Tumour necrosis factor alpha (TNF-α), and monocyte chemoattractant protein 1 (MCP-1) liver mRNA levels were quantified by real-time PCR. Mink fasted for 5 and 7 days had significantly higher levels of TNF-α and MCP-1 liver mRNA, compared to mink fasted for 0, 1, and 3 days. Mink fasted for 7 days, but re-fed for 28 days had the lowest mRNA levels of both TNF-α, and MCP-1 demonstrating the liver's ability to restore homeostasis post-fasting. TNF-α mRNA levels were correlated with MCP-1 liver mRNA and liver fat percent. To confirm the physical presence of inflammation, slides stained with haematoxylin and eosin were analyzed for bile ducts resulting in no significant differences. Results indicate that elevated MCP-1 and TNF-α expression are associated with fasting induced fatty liver in mink.

LIST OF ABBREVIATIONS USED

ACC-1	Acetyl-COA carboxylase-1
ACTH	Adenocorticotropic hormone
ALD	Alcoholic liver disease
BEC	Biliary endothelial cells
CAM	Cell adhesion molecules
CCL2	Chemokine (C-C motif) ligand 2
CCR2	C-C chemokine receptor 2
CDAA	Choline deficient amino acid-defined
cDNA	Complementary deoxyribonucleic acid
CPT1	Carnitine palmitoyltransferase 1
CRP	C-reactive protein
DNA	Deoxyribonucleic acid
DNL	*De novo* lipogenesis
ECM	Extracellular matrix
FA	Fatty acid
FAS	Fatty acid synthase
FFA	Free fatty acid
FGF	Fibroblast growth factor
FIHL	Feline idiopathic hepatic lipidosis
GAPDH	Glyceraldehyde-3-phosphate dehydrogenase
GLUT-4	Glucose transporter-4
H-MRS	Magnetic resonance spectroscopy
HSC	Hepatic stellate cell
IGF-1	Insulin-like growth factor 1
IL-1	Interleukin-1
IL-6	Interleukin-6
IL-8	Interleukin-8
IRS-1	Insulin receptor substrate 1
mRNA	Messenger ribonucleic acid
MCP-1	Monocyte chemoattractant protein-1 Monocyte chemotactic protein-1
MUFA	Monounsaturated fatty acid
NAFLD	Non-alcoholic fatty liver disease
NAI	NASH activity index
NAS	NAFLD activity score
NASH	Non-alcoholic steatohepatitis
NO	Nitric oxide
PCR	Polymerase chain reaction
PPAR-α	Peroxisome proliferator-activated receptor alpha
PUFA	Polyunsaturated fatty acid
qRT-PCR	Quantitative real time polymerase chain reaction
RF	Re-fed
RNA	Ribonucleic acid
ROS	Reactive oxygen species

SEC	Sinusoidal endothelial cells
SEM	Standard error of mean
SFA	Saturated fatty acid
SREBP-1	Sterol regulatory element-binding protein 1
TAG	Triacylglycerol
TG	Triglycerides
TNF-α	Tumour necrosis factor alpha
UFA	Unsaturated fatty acid
VLDL	Very low density lipoproteins
WT	Wild-type

ACKNOWLEDGEMENTS

I would first like to extend my gratitude towards my supervisor Dr. Kirsti Rouvinen-Watt for her support and continued patience during the completion of my studies. I would also like to acknowledge my committee members Dr. Lori Parsons and Dr. Vasantha Rupasinghe for their time and commitment to my project. Completion of this project would not have been possible without the expertise and guidance from Lora Harris. Thank you Lora for all of your help, you are truly irreplaceable. I would like to thank Catherine Pal for her GAPDH data and also Dr. Tessema Astatkie for his statistical guidance. This research was funded by the Nova Scotia Department of Agriculture Technology Development Program (DEV27-066), Canada Mink Breeders' Association and the Natural Sciences and Engineering Research Council of Canada (Discovery Grant to KRW).

I want to thank my family and particularly my parents for their unconditional support of my decisions in life as none of this would be possible without them. I want to specifically thank my mother for continually motivating me to be the best that I can be and my father for demonstrating the work ethic required to become successful in life. I hope I have made you both proud.

CHAPTER 1.0 INTRODUCTION

A common problem among mink ranchers is the impact of disease with forty-five percent of ranchers in North America having occurrences of nursing sickness (Rouvinen-Watt and Hynes 2004). Nursing sickness is the largest cause of death among breeder females and is very costly to ranchers (Rouvinen-Watt 2003). Nursing sickness occurs towards the end of lactation, or near the start of weaning, and is characterized by weight loss, anorexia, lethargy, and dehydration (Clausen *et al.* 1992; Nieminen *et al.* 2009). Upon gross necropsy of dams varying degrees of hepatic lipidosis have been reported (Seimiya *et al*. 1988). In mink, the pathogenesis of hepatic lipidosis is similar to that of the development of non-alcoholic fatty liver disease (NAFLD) (Adams *et al.* 2005), alcohol-induced fatty liver disease (Seth *et al.* 2011), and feline idiopathic hepatic lipidosis (FIHL)(Griffin 2000). In 2010, Rouvinen-Watt *et al*. demonstrated in a mink model that hepatic lipidosis could also be induced through periods of fasting. Currently there are no definitive diagnostic tests for hepatic lipidosis, however, the most accurate medical method for diagnosis is liver biopsy accompanied with histological evaluation (Brunt *et al.* 2009). The development of assays capable of detecting proteins secreted during the progression of inflammation associated with fatty liver disease may enable a non-invasive diagnosis, which would be valuable to the research and veterinary medical community.

Fatty liver disease is defined as the transitioning from the more benign steatosis, to steatohepatitis, and finally to the development of fibrosis and cirrhosis (Farrell and Larter 2006). The transition from simple steatosis to steatohepatitis is characterized by the presence of inflammation demonstrated by the infiltration of immune cells within the

liver tissue, which is provoked by the secretion and binding of proteins, specifically cytokines and chemokines (O'Shea and Murray 2008). Two proteins that are believed to be involved in the development of steatohepatitis are tumour necrosis factor alpha (TNF-α), and monocyte chemoattractant protein-1 (MCP-1). The purpose of this study is to quantify the presence of TNF-α and MCP-1 liver mRNA expression levels in correlation with liver fat percent via quantitative real time polymerase chain reaction (qRT-PCR). From a morphological perspective, an increased number of bile ducts have been implicated with the fibrous progression of NAFLD, thus bile ducts were quantified per field of view to determine if a similar relationship is present in mink (Sasaki *et al*. 2010). The results of this research will enable a better understanding of the effects of fasting-induced fatty liver on the development of liver inflammation in the mink.

CHAPTER 2.0 LITERATURE REVIEW

2.1 Mink and the industry

In 2009, Nova Scotia produced over 825 000 mink pelts accounting for more than half of Canada's total pelt production for the year resulting in the industry being one of the province's largest agricultural sectors (Statistics Canada 2011). A common problem among mink ranchers is the impact of disease leading to the loss of breeder females. Nursing sickness is the largest cause of death in female mink and is accompanied with the development of hepatic lipidosis, which is associated with seasonal body weight fluctuations (Nieminen *et al*. 2001; Rouvinen-Watt 2003). There are several periods during the production year when breeder females are at risk for the development of hepatic lipidosis. In autumn, ranchers increase feeding to enable mink to gain maximum body weight, which results in a larger pelt size (Korhonen and Niemelä 1997). During the late winter months conditioning of females prior to the breeding season leads to rapid body weight loss while increasing chances of successful mating (Clausen *et al*. 1992; Bjornvad *et al.* 2004). Finally female mink are at an increased risk during parturition, late lactation, or toward the early stages of weaning due to an increase in energy demand (Schneider and Hunter 1993). Ranching protocols promote a continual increase in production, which results in large metabolic demands on breeder females increasing the risk of developing fatty liver. This represents a loss that can be potentially prevented.

2.2 Mink nursing sickness and fatty liver disease in carnivores

The development of fatty liver disease associated with nursing sickness in mink has a measurable impact on the mink industry. Nursing sickness occurs towards the end

of lactation, or within the first week of weaning, and is associated with the increase in energetic demands of lactation (Clausen *et al.* 1992; Rouvinen-Watt 2003). The incidence of nursing sickness varies among farms, but may reach as high as 15% (Hunter and Lemieux 1996). In a North American survey, forty-five percent of ranchers reported having problems with nursing sickness (Rouvinen-Watt and Hynes 2004). The development of fatty liver disease may occur sporadically and is associated with a genetic predisposition for the development of nursing sickness (Rouvinen-Watt 2003). Bjornvad and colleagues (2004) found that short-term fasting of mink resulted in accumulation of intra-hepatic lipid vacuoles resulting in liver weight remaining the same, while body weight decreased. In 2010, Rouvinen-Watt *et al*. fasted mink for 0-7 days resulting in an increase in intra-hepatic triacylglycerols (TAG), an increase in liver fat percent, and a decrease in n-3 polyunsaturated fatty acids (PUFA), while re-feeding reversed these changes. Persson and associates (2011) found that seasonal body weight fluctuations in wild male mink correlated with an increase in liver weight, which was associated with an increase in liver fat percent. Fatty liver disease not only affects mink, but also other species as well. Another Mustelid, the European polecat has been documented to possess a similar fatty acid (FA) profile to that of humans when hepatic lipidosis is induced through food deprivation (Nieminen *et al.* 2009). This study concluded that mustelids may in fact present a novel model for the pathogenesis of fatty liver disease in humans. In domestic cats, Griffin (2000) reported that 49% of 175 feline liver biopsies confirmed FIHL. In cats that were >40% overweight, Biourge and associates (1994) found that long term fasting for 5 to 7 weeks resulted in hepatic lipidosis indistinguishable from FIHL. In 1998, Nicoll *et al*. used ultrasonography to determine that obese male cats developed

fatty liver once fed *ad libitum* or when under a severe diet restriction. In these carnivores rapid body weight loss, obesity, severe diet restriction, and short-term fasting all lead to the development of fatty liver.

2.3 Non-alcoholic fatty liver disease

NAFLD is a term that encompasses a full range of liver diseases progressing from simple steatosis to steatohepatitis, and fibrosis ending with cirrhosis (Farrell and Larter 2006). NAFLD is primarily associated with the development of insulin resistance as part of the many metabolic changes that occur during the progression of obesity, type II diabetes, metabolic syndrome, hypertension and dyslipidemia (Hamaguchi *et al*. 2012). Diagnosis of NAFLD has quickly increased in parallel with the rise in levels of obesity and diabetes, resulting in NAFLD becoming the most common form of liver disease in the Western world (de Alwis and Day 2008; Vuppalanchi and Chalasani 2009). In Western populations the estimated incidence of NAFLD varies between 20 and 30%, while non-alcoholic steatohepatitis (NASH) affects 2-3% of the general population (Bedogni *et al*. 2005; Browning *et al*. 2004). The most prevalent risk factors are male gender, age, obesity, and insulin resistance (Bellentani *et al.* 2010).

Simple steatosis is characterized by the accumulation of TAG in liver cells until fatty tissue accounts for greater than 5% of the total liver weight and may be zone 3 predominant (Brunt *et al.* 2009). The progression of simple steatosis to steatohepatitis is currently characterized by the infiltration of immune cells into liver tissue, ballooning of hepatocytes, and fibrosis (Chalasani *et al.* 2008). Steatosis is relatively benign, while steatohepatitis can progressively lead to severe fibrosis and cirrhosis of the liver. When

fibrosis develops the deposition of collagen occurs initially in the perisinusoidal space of Disse and in zone 3, progressing to portal and periportal fibrosis (Brunt *et al.* 2009).

Despite recent advances in the understanding of the pathogenesis of NAFLD, uncertainties still exist pertaining to the metabolic and inflammatory pathways involved with the progression from steatosis to cirrhosis. Preliminary theories for the development of NASH are centralized around the idea of a two-hit hypothesis and recently a third-hit has been proposed (Day 2006, Dowman *et al.* 2010). The first-hit was defined as the accumulation of hepatic TAG leading to steatosis, followed by the second-hit involving cytokine/chemokine mediated inflammation, mitochondrial dysfunction, and oxidative stress. The third-hit involves the liver's inability to regenerate due to oxidative stress hindering hepatocyte proliferation and differentiation from oval progenitor cells resulting in hepatocyte death (Downman *et al.* 2010). The three-hit hypothesis has since been modified to incorporate the effect of free fatty acids (FFA) in the progression of liver injury. The development of obesity and insulin resistance results in an increase of FFA into the liver, which are either broken down via β-oxidation, exported by lipoproteins, or stored by esterification (Feldstein *et al.* 2004). Recently the liver saturated fatty acids (SFA)/unsaturated FA (UFA) ratio has been associated with lipotoxicity since NAFLD results in the impairment of oxidizing and exporting SFA leaving storage as the only option (Gormaz *et al.* 2010; Trauner *et al.* 2010). Li and associates (2009) have indicated that the desaturation of SFA into mono-unsaturated fatty acids (MUFA) has a protective effect of removing the cytotoxic SFA, but leads to a more advanced disease progression due to the increasing fat accumulation hindering basic liver function. In mink from this study, Rouvinen-Watt *et al.* (2012) demonstrated that acetyl-CoA carboxylase-1 (ACC-1)

and fatty acid synthase (FAS) messenger ribonucleic acid (mRNA) expression levels were increased after fasting mink for 5-7 days of fasting. This suggests that hepatic *de novo* lipogenesis (DNL) further exacerbates the development of fatty liver. The increase in DNL results in the synthesis of C16 and C18 SFA, which are capable of being desaturated into MUFAs and were found to be higher in the fasted mink (Rouvinen-Watt *et al.* 2012).

2.4 The liver

2.4.1 Organization

The liver is the largest internal organ accounting for an average 2.5% of human adult body weight and 2-3% of adult mink body weight depending on the time of year (Mustonen *et al*. 2005; Ross and Pawlina 2006). The human liver is divided into four lobes, while in the mink liver consists of five lobes, the right median and lateral, the left median and lateral, and the quadrate (Smith and Schenk 1999). Blood is supplied to the liver from two sources, the hepatic portal vein and hepatic artery. The hepatic vein carries de-oxygenated blood containing nutrients, xenobiotics, blood cells, and endocrine secretions from other tissues of the body, while the hepatic artery provides oxygen rich blood (Haüssinger 1990). Liver lobes are comprised of hepatic lobules, which are composed of organized plates of hepatocytes called parenchyma (Baratta *et al*. 2009). Hepatic lobules are surrounded by portal triads, which contain a bile duct and supplies blood from both the hepatic artery and portal vein. Sinusoidal capillaries separate the anastomosing plates of hepatocytes and bathe the hepatic cells in blood enabling liver function. There are three structural models that currently explain the functions of the liver consisting of the classic lobule, portal lobule, and liver acinus (Ross and Pawlina 2006).

The classic lobule model is hexagonal in shape and blood flow radiates from the portal triads to the central vein, while the portal lobule forms a triangle with an inner portal triad leaving blood flowing towards a central vein in each corner. The liver acinus model involves three zones located between two classic lobules with an oxygen gradient descending towards zone three resembling a diamond shape (Rappaport *et al*. 1983).

2.4.2 Functions and cellular structure

The liver plays many important roles in the regulation of homeostasis. These include the uptake, storage, and distribution of nutrients and vitamins, maintenance of glucose levels, regulation of very low-density lipoproteins (VLDL), degradation or conjugation of xenobiotics and drugs, secretion of bile, and endocrine functions (Leevy *et al.* 1970; Evans *et al*. 1976; Nagelkerke *et al.* 1983; Ross and Pawlina 2006; Baratta *et al*. 2009). These functions are performed by the coordination of all hepatic cells.

2.4.2.1 Hepatocytes

Hepatocytes comprise nearly 75% of all liver cells and the average lifespan is five months (Ross and Pawlina 2006). Hepatocytes form plates lining the sinusoid and come in direct contact with nutrients, toxins, and endocrine secretions contained in the blood. Hepatocytes perform many functions including 1) metabolism of xenobiotics via cytochrome P450s, 2) synthesis of plasma proteins, 3) production of bile salts, and 4) storage of iron as a ferritin complex (Smedsrød *et al.*1990; Sellaro 2008). It has been recognized that both under normal and pathological conditions many hepatocyte functions are regulated by proteins released from neighboring non-parenchymal cells.

2.4.2.2 Sinusoidal endothelial cells

Sinusoidal endothelial cells (SECs) constitute 70% of the sinusoidal cells in the liver and form a fenestrated barrier between the blood and hepatocytes (Katz *et al.* 2004; Smedsrød *et al.*1990). SECs have been implicated in the clearance of modified or denatured proteins, excess extracellular matrix (ECM) components including hyaluronic acid, lipoproteins, and denatured collagen by receptor mediated endocytosis (Enomoto *et al.* 2004). SECs play an important role in the inflammatory response of the liver. Chemical stimulation induces SECs to express cell adhesion molecules (CAMs) that mediate extravasation of immune response cells into target tissues (Essani *et al.*1995).

2.4.2.3 Stellate/Ito cells

Hepatic stellate cells (HSCs) also known as Ito cells were discovered by Von Kupffer in 1876 and are located in the perisinusoidal space of Disse of the liver (Winua *et al.* 2008). The non-immunological functions of HSCs centralize around the storage of 80% of the bodies' total vitamin A as retinyl palmitate, transport of retinoids, secretion of ECM components, and regulation of hepatic blood flow (Senoo 2004). The structure of HSCs change upon fibrotic conditions altering phenotypes from a star-like cell to a spindle-like myofibroblast with increases in endoplasmic reticulum and Golgi apparatus development (Senoo 2004). HSCs are activated by TNF-α and fibroblast growth factor (FGF) (Kisseleva and Brenner 2006). Activation enables HSCs to secrete pro-inflammatory cytokines resulting in an up-regulation of CAMs expression, which further accelerates an immune response. HSCs secrete the chemokine MCP-1 signaling macrophage recruitment.

2.4.2.4 Kupffer cells

Kupffer cells comprise approximately 80-90% of the bodies' resident macrophage population and may persist for weeks or up to 14 months (Bilzer *el al.* 2006). Kupffer cells reside in the sinusoids of the liver and the concentration, size, and phagocytotic capability of each individual Kupffer cell depends on location within the liver acinus (Odegaard *et al.* 2008). Kupffer cells play a pivotal role in the body's innate immune defense by dealing with the clearance of particulate and exogenous materials from the portal circulation and endogenous signals that are a result of disturbances in homeostasis (Baffy 2009). Both endogenous and exogenous threats are capable of activating Kupffer cells leading to a series of actions. Kupffer cells are able to 1) launch a biochemical attack stimulating interactions with other liver cells via cytokines, chemokines, prostaglandins, reactive oxygen species (ROS), proteolytic enzymes and nitric oxide (NO) (Neyrinck *et al.* 2009; Clària *et al.* 2011), 2) initiate an inflammatory response by recruiting leukocytes via expressing CAMs and releasing chemokines, 3) phagocytose, digest and eliminate solid particles (Baffy 2009); and 4) contribute to adaptive immunity by processing antigens to attract cytotoxic and regulatory T-cells. Thus, Kupffer cells are a key regulatory cell in the liver and are highly influential in the pathogenesis of inflammation.

2.5 Inflammation

2.5.1 Acute inflammation

The acute phase response is an organism's reaction to disturbances in homeostasis that can be triggered by numerous factors including infection, tissue damage, neoplastic

growth, or immunological disorders (Gabay 2006). Tissue injury is accompanied with an increase in vascular diameter, but a decrease in blood flow (Heinrich *et al.* 1990). The increased volume results in vascular permeability enabling fluid to enter the damaged tissue. Furthermore, accumulation and activation of both granulocytes and mononuclear cells, along with the activation of endothelial cells leads to secretions of cytokines resulting in a systemic response (Kindt *et al.* 2007). An acute systemic response results in the induction of fever, leukocytosis, erythrocyte sedimentation, increased secretion of adrenocorticotropic hormone (ACTH) and glucocorticoids, negative nitrogen balance, and secretion of acute phase protein including C-reactive protein (CRP) (Heinrich *et al.* 1990).

Many systemic acute phase effects are due to the combined action of TNF-α, IL-6 (Interleukin-6), and IL-1 (Interleukin-1; Gabay 2006). The launch of an acute inflammatory response is characterized by neutrophil infiltration in the tissue of injury. Neutrophils produced by bone marrow travel in the blood until certain CAMs have been activated or expressed. TNF-α and IL-1 increase expression of E-selectin which binds to mucins present on neutrophils beginning the process of rolling (Kindt *et al*. 2007). Rolling is the first step in the process of extravasation, which involves the exit of fluid from a blood vessel into the surrounding tissue. The process of extravasation associated with an acute response is a critical step in the progression of hepatic lipidosis (Ramaiah and Jaeschke 2007). The infiltration of lipids in the liver hinders basic function resulting in the triggering of an acute inflammatory response to restore homeostasis.

2.5.2 Chronic inflammation

Chronic inflammation is characterized by the change from neutrophil to monocyte infiltration (Heinrich *et al.* 1990). Monocyte infiltration is triggered by changes in chemokine secretion. TNF-α and IL-1 are capable of stimulating endothelial cells to secrete IL-8, IL-6 and increase expression of CAMs (Elias and Lentz 1990). During neutrophil infiltration, shredding of the membrane releases the soluble IL-6 receptor sIL-6Rα (Gabay 2006). The binding of IL-6 and sIL-6Rα to gp130 on the surface of endothelial cells terminates the secretion of IL-8 and increases the secretion of MCP-1. This transition period requires the clearance of neutrophils. Neutrophils are crucial in host defense via their ability to synthesize oxygen metabolites and enzymes (Vissers and Hampton 2004). These substances can be toxic to surrounding tissues, thus apoptotic neutrophils express new membrane antigens that attract macrophages. Phagocytosis of neutrophils leads to an increased expression of MCP-1 from macrophages and a decrease in IL-8 (interleukin-8) from neutrophils (Heinrich *et al.* 1990). As neutrophils are cleared from the inflammatory site, monocytes continue to infiltrate resulting in differentiation into inflammatory macrophages (Rydell-Törmänen *et al.* 2006). These cells then may present antigenic peptides that may recruit lymphocytes further exacerbating the immune response. Chronic inflammation occurs when the acute phase response persists to a point where more severe measures must be taken to restore homeostasis (Gabay 2006). The progression of hepatic lipidosis to a stage where monocyte infiltration occurs is mediated by the secretion and binding of inflammatory proteins.

2.6 Cytokines

In order to launch an immune response, there must be communication among lymphoid, inflammatory and hematopoietic cells (Kindt *et al.* 2007). Communication is accomplished by the secretion and binding of proteins, specifically cytokines (O'Shea and Murray 2008). Cytokines are released after a cell is stimulated by a specific cue and may act in an autocrine, endocrine or a paracrine fashion (Coppack 2001). They bind to particular receptors on the membrane of target cells, which results in a signal transduction pathway that leads to a change in expression of certain genes (Wormald and Hilton 2004). Cytokines are capable of synergistic, antagonistic, redundancy and cascade effects that permit regulation of cellular processes in a coordinated manner (Kindt *et al*. 2007). A cytokine believed to have implications with the inflammation involved with fatty liver disease is TNF-α.

2.6.1 *TNF-α*

In 1984, two different TNFs were isolated and discovered to be cytotoxic to tumour cells in mice resulting in regression of the tumour (Aggarwal 2003). Research during the last 20 years has increased the TNF superfamily to 19 proteins signaling through 29 receptors including TNF-α. TNF-α is a proinflammatory cytokine that plays a central role in the innate and adaptive immunity, cell proliferation, and apoptotic processes (Popa *et al.* 2007). TNF-α is produced by a variety of cells throughout the body including macrophages, monocytes, adipocytes, and endothelial cells (Antuna-Puente *et al.* 2008). There are two different types of TNF-α receptors that are present on every cell membrane with the exception of erythrocytes, TNF-α-R1 and TNF-α-R2 (Popa *et al.*

2007). The two receptors differ in their binding affinity of TNF-α and in addition to their signaling pathways. Increased concentrations of TNF-α have been implicated in the progression in many diseases including type II diabetes and the metabolic syndrome (Yang *et al.* 2009).

TNF-α is a pleiotropic cytokine that has many important roles in both inflammation and metabolism (Popa *et al.* 2007). During situations of increased plasma TNF-α, most diseases are also accompanied with an increase in plasma TAG leading to hypertriglyceridemia (Hotamisligil *et al.* 1995). TNF-α induces hypertriglyceridemia by five distinct ways, 1) increasing FFA production from both adipose tissue and liver, 2) diminishing clearance of VLDL from the liver, 3) decreasing expression of apoE in hepatocytes resulting in TAG rich lipoproteins in circulation for a longer period of time, 4) increasing *de novo* FA synthesis by increasing levels of hepatic citrate, and 5) TNF-α alters the phenotypic state of pre-adipocytes resulting in the inability to store lipids properly activating a local and systemic inflammatory response. As a result TNF-α has the ability to shift lipid metabolism from a state of equilibrium to a condition where excess synthesis and release along with a decrease in transport efficiency leads to a surplus of TAG in circulation.

TNF-α is capable of not only hindering lipid metabolism, however it hinders glucose metabolism as well. TNF-α influences insulin signaling by interfering with the insulin receptor substrate-1 (IRS-1) causing a serine phosphorylation (Matsuzawa 2005). In adipose tissue, TNF-α stimulates lipolysis causing an increase in plasma FFAs leading to insulin resistance and an increase in glucose production from the liver (Hotamisligil *et al.* 1995). TNF-α plays a pivotal role in the production of many other cytokines and is

able to induce insulin resistance by generating a down-regulation of adiponectin and an increased expression of leptin (Trayhurn and Wood 2005). Stimulation of MCP-1 release by TNF-α leads to an inflammatory response that generates insulin resistance (Smith *et al*. 2007). Overall, TNF-α has a multitude of effects that severely impair lipid and glucose metabolism.

2.7 Chemokines

Another group of proteins associated with cell signaling are chemokines. Chemokines affect the chemotaxis of leukocytes and play an important role in the inflammatory response. The most important chemokine relating to the transition from NAFLD to NASH is MCP-1.

2.7.1 *Monocyte chemoattractant protein-1*

Chemokines consist of four classes depending on the position of conserved cysteine (CC) residues and are also known as conserved cysteine ligands (Marra *et al.* 1998). MCP-1 belongs to the CC class 2 (CCL2) and determines recruitment and activation of monocytes and T-lymphocytes. MCP-1 is secreted by a variety of cells including endothelial, Kupffer, and hepatic stellate cells. Presence of MCP-1 is involved with the progression of many diseases including hepatic lipidosis. MCP-1 plays an important role in the development of inflammation associated with the transition from simple steatosis to NASH and there is a positive relationship between an increase in obesity and MCP-1 levels (Haukeland *et al.* 2006). Weisberg and associates (2006) discovered that in diet-induced obese mice; an absence of the C-C motif chemokine

receptor-2 (CCR2), which regulates monocyte/macrophage recruitment, protects the liver against accumulation of lipids. Using rats with a mutated CCR2 suppressing receptor activity, Imamura *et al.* (2005) found that dimethylnitrosamine-induced infiltration of macrophages and lymphocytes into liver tissue was suppressed, activation of HSC was eliminated, and fibrogenesis was prevented. Similar results have been obtained in humans as MCP-1 is over-expressed in the adipose tissue of individuals that are insulin resistant, which is accompanied with an accumulation of macrophages (Westerbacka *et al.* 2007). Overall, the morphological changes of the liver during the development of fatty liver bear significant similarities to those that occur to adipose tissue during obesity, indicating that an adipogenic transformation may be occurring in the liver (Westerbacka *et al.* 2007). Using the same mink from this study, Rouvinen-Watt and associates (2012) have demonstrated an increase in hepatic DNL, which is suggested to be caused by an adipogenic transformation of the hepatocytes. Similar to changes seen in humans with NAFLD, the liver expresses gene profiles normally expressed in healthy adipose tissue (Westerbacka *et al.* 2007).

2.8 Diagnosis and liver histology

NAFLD is most often diagnosed in patients that have elevated aminotransferase levels found in routine exams since there are no causal symptoms associated with the disease (Farrell and Larter 2006). Testing for fatty liver involves analyzing blood and urine, along with radiographic findings that may be indicative of NAFLD, but the most accurate medical method of differentiating between steatosis and steatohepatitis is liver biopsy accompanied with histological evaluation (Brunt *et al.* 2009). Liver biopsy is

expensive, carries risks to patients, and practitioner diagnoses vary from one to another leading to poor reproducibility and large sampling variability. When a liver biopsy is performed a small fragment of liver is removed, which is estimated to represent 1:50 000 of the whole organ (Raitziu *et al.* 2007). In most chronic liver diseases it has been recognized that the distribution of histological lesions is variable indicating that a single sample may lead to invalid diagnosis (Bravo *et al.* 2001).

In 1999, Brunt and associates developed a semi-quantitative system to grade NASH, while Matteoni and colleagues (1999) developed a grading system to define NAFLD. The scoring system was based on characteristics relating to steatosis, ballooning of hepatocytes, lobular and portal inflammation. Recently Kleiner and colleagues (2005) created the NAFLD activity score (NAS) focusing on steatosis, lobular inflammation, and hepatocyte ballooning. NAS was designed to validate the presence of NASH with reasonable inter-rater reproducibility, but has become a scoring system for NAFLD. In 2010, Merat and associates continued to develop the scoring system, but with an emphasis on NASH. The NASH activity index (NAI) was created focusing on all four characteristics proposed by Brunt *et al.* (1999) since portal inflammation has been deemed to be critical in NASH development.

2.8.1 Lobular and portal inflammation

Lobular inflammation is defined as the presence of inflammatory lymphocytes in the sinusoids of the liver (Brunt 2005). It is associated with the development of mixed acute and chronic inflammatory infiltrates, which accumulate in the lobules of the liver in response to stress (Caballero *et al.* 2012). In contrast, portal inflammation is described as

the infiltration of a more chronic inflammatory cell population surrounding the portal triads and central veins of the liver (Brunt *et al*. 2009, Rakha *et al.* 2010). Chronic cells involved are lymphocytes, plasma cells, occasional eosinophils, and monocytes. The presence of these cells in the liver is an end result of an accumulation of liver lipids.

2.8.2 Microvesicular versus macrovesicular steatosis

Steatosis has been classically identified as macrovesicular or microvesicular (Yerian 2011). Macrovesicular and mixed steatosis are more commonly diagnosed than microvesicular steatosis. Macrovesicular steatosis has been consistently associated with fatty liver disease and the metabolic syndrome, but also stimulated by starvation and rapid body weight loss in obese people (Schwimmer *et al*. 2006). Macrovesicular steatosis is characterized by the presence of few well-defined fat droplets present in the hepatocyte cytoplasm displacing the nucleus to the cell's periphery (Mofrad and Sanyal 2003). In comparison, microvesicular steatosis is rare and is frequently associated with severe clinical illnesses involving mitochondrial and hepatic dysfunction (Marion *et al* 2004). Microvesicular steatosis is defined by the presence of numerous fat droplets that are smaller than the cells nucleus, giving the cytoplasm a foamy appearance (Liquori *et al.* 2009). The presence of either or both forms of steatosis results in an increase in cell size and serves as a defining characteristic in determining the progression of NAFLD.

2.8.3 Hepatocyte ballooning

Ballooning is a feature that was first described by Matteoni and colleagues (1999) and has been used as clinical characteristics for positive diagnoses of NAFLD. The term

ballooning refers to the hepatocytes enlarging in size and can be sometimes associated with the development of Mallory's hyaline (Brunt 2004). Hepatocyte ballooning is caused largely by the development of steatosis leading to microtubular disruption and cellular injury resulting in necrosis.

2.8.4 Bile ductular proliferation

Division of mature hepatocytes and/or cholangiocytes in the adult liver drives normal tissue homeostasis and regeneration after hepatocellular or biliary damage (Strazabosco and Fabris 2012). Recently, an increased number of bile ductules have been implicated with the fibrous progression of various chronic liver diseases including NAFLD (Sasaki *et al*. 2010). Chiba and associates (2011) found a positive relationship between the number of bile ductules and NAFLD disease progression. Bile ductules are composed of biliary endothelial cells (BEC). BECs are found to induce cellular senescence and express MCP-1, which is related to periportal and portal fibrosis and inflammation.

2.9 Conclusion

The liver is one of the most important organs in the maintenance of homeostasis. Along with the rise in obesity is an increase in the occurrence of fatty liver disease. In mink, fatty liver is a common cause of death among breeder females and represents a large annual loss for farmers. The development of fatty liver is asymptomatic and leaves a very narrow window for intervention. Currently the only effective method of detecting fatty liver disease is via liver biopsy. In mink, biopsies are not a logical practice since the shaving of fur during winter would hinder the animal's ability to properly thermoregulate

and the value of the biopsy in relation to the value of the animal is cost-prohibitive. The development of inflammation related to the progression from steatosis to steatohepatitis represents a novel approach for detection of fatty liver. Inflammation requires the coordination of many cytokines and chemokines in order to restore homeostasis. The roles of TNF-α and MCP-1 in the development of inflammation render them ideal candidates for the monitoring of disease progression in NAFLD. Identification of these critical markers as indicators of inflammation in the development of fatty liver in post-mortem samples will promote further research on the detection of these proteins in live animals. This will in turn increase the potential of early diagnosis of this disease.

CHAPTER 3.0 OBJECTIVES AND HYPOTHESES

The overall objectives of this research were to characterize the pathogenesis of inflammation in the fatty liver in fasted mink by quantifying TNF-α and MCP-1 liver mRNA expression levels, and determining the physical presence of inflammation through histological analysis. It is hypothesized that there will be no difference in liver messenger ribonucleic acid expression levels of TNF-α or MCP-1 between sexes. There will be an increase in TNF-α liver mRNA expression peaking in mink fasted for five days, while there will be an increase in MCP-1 liver mRNA expression peaking in mink fasted for seven days. Histological examination will support these hypotheses with mink fasted for 5 and 7 days having more bile ducts present per foci. Mink re-fed (RF) for 28 days will return to control liver mRNA expression levels of TNF-α and MCP-1, while RF mink will have similar amounts of bile ducts present as control treatments.

CHAPTER 4.0: MATERIALS AND METHODS

4.1 Fasting trial

Sixty (60) 9-month-old standard black mink were used in the fasting trial. Treatment groups consisted of 5 males and 5 females, which were fasted for 0, 1, 3, 5 or 7 days. In addition a re-feeding (RF) treatment was carried out where 5 males and 5 females were fasted for 7 days followed by *ad libitum* feeding for 28 days. The fasting regimes were conducted from January 9th to 16th 2007 and the re-feeding was carried out from January 16th to February 13th 2007. The mink were weighed, anaesthetized, sampled for blood, and euthanized at the end of each experiment. Livers were excised, gall bladders removed, weighed, and snap-frozen in liquid nitrogen prior to being stored in an -80º freezer. All experimental procedures were approved by the Animal Care and Use Committee of the Nova Scotia Agricultural College and were carried out in accordance with the guidelines of the Canadian Council for Animal Care, ACUC file no. 2006-089. For further details see Rouvinen-Watt *et al*. (2010).

4.2 Quantitative real time polymerase chain reaction assays

4.2.1 Ribonucleic acid extraction

Total ribonucleic acid (RNA) was extracted from liver tissue via the RNeasy® Mini Kit with DNase-l digestion as per manufacturer's protocols (QIAgen, Valencia, CA, USA). Liver samples were removed from storage and placed in liquid nitrogen, 20-30mg of tissue was separated, and Buffer RLT with 2-mercaptoethanol was added to prevent RNA degradation. A Kontes Pellet Pestle® micro grinder (Kimble, Vineland, NJ, USA) was used to mechanically homogenize liver tissue, while the high molecular weight

cellular components were homogenized with a QIAshredder (QIAgen, Valencia, CA, USA). RNA was then isolated by applying the homogenized lysate to a spin column with equal parts of 50% ethanol followed by a wash with RW1. The column was then incubated with DNase-1 for 15 minutes to remove genomic deoxyribonucleic acid (DNA) contaminants. The column was washed with Buffer RPE and 70% ethanol for a total of 3 washes. RNA was eluted twice, first with 30µl of RNAse free water and then the eluate from the first spin. RNA quality and quantity was assessed via a 260/230 (salt and ethanol contamination) and 260/280 (protein contamination) ratios of minimum 1.8 attained from a NanoDrop 1000 spectrophotometer (Fisher Scientific, Ottawa, ON, CAN), a 28S to 18S ratio of minimum 1:1 via a 0.7% agarose gel, and no reverse transcription controls.

4.2.2 Complementary deoxyribonucleic acid synthesis

RNA was reverse transcribed using a High Capacity (cDNA) Reverse Transcription Kit (ABI, Carlsbad, CA, USA) including a MultiScribe™ Reverse Transcriptase according to manufacturer's protocols. A 2X Mastermix was prepared with an equal volume of 1.0µg RNA in 20µl aliquots and was pipetted into 8-well strips. The 8-well strips were run in the Dyad® Peltier Thermal Cycler (Bio-Rad, Mississauga, ON, CAN) for 10 minutes at 25°C, 120 minutes at 37°C, 5 seconds at 85°C, and held at 10°C until termination of the program. cDNAs were aliquoted into 0.1X and 0.01X dilutions using 10mM Tris-Cl, pH 7.4 and stored at -30°C.

4.2.3 Sequencing

Sequences were attained firstly by searching existing databases and secondly by designing primers based off homologies present between similar species as follows.

4.2.3.1 Monocyte chemoattractant protein-1

MCP-1 sequence was designed using homologies between ferret, dog, cat, human, mouse, and horse sequences attained from GenBank (Table 1). Sequences were aligned using BioEdit Sequence Alignment Editor (Copyright © 1997-2007 Tom Hall Version 7.0.9.0; Hall 1999) followed by the designing of primers via Primer 3 version 0.4.0 (Rozen and Skaletsky 2000). Primer 3 parameters were product size range of 400-800, table of thermodynamic parameters set to Santa Lucia 1998, max 3' self-complementarity at 0, max poly X at 3, salt correction formula set to Santa Lucia 1998, concentration of divalent cations at 2.5, and concentration of dNTPs at 0.2. Primers were ordered from Sigma® Life Science (Sigma-Aldrich, Oakville, ON, CA) and were tested via polymerase chain reaction (PCR) with a 48-68°C annealing temperature gradient using the Dyad® Peltier Thermal Cycler (Bio-Rad, Carlsbad, CA, USA). PCR parameters consisted of a hot start at 94°C for 5 minutes followed by 30 cycles of 94°C, a gradient from 48-68°C, and 72°C each for 30 seconds, incubated at 72°C for 6 minutes, and held at 10°C until the program was terminated. Preliminary sequence was attained from the primers F89 and R309 yielding a product size of 221 base pairs (Table 2). The reaction mix contained Ultrapure^{TM} DNase/RNase-free distilled water, 1X PCR buffer containing 200 mM Tris-HCl (pH 8.4) and 500 mM KCl, 1.5 mM $MgCl_2$, 0.2 mM GeneAmp dNTP mix, 0.24 μM forward primer MCP1 F89, 0.24 μM reverse primer MCP1 R309, 0.8 U

Taq DNA polymerase, and 8µl of 1X FL07 liver cDNA. A 2% agarose gel electrophoresis was used to confirm a single band of the desired size. Primers MCP1 F20 and MCP1 R320 were designed to extend the sequence on the 3' end and the PCR product resulted in a single band at an annealing temperature of 58°C, which was then purified using Montage PCR-50 columns (Fisher Scientific, Ottawa, ON, CAN; Table 2). PCR parameters consisted of a hot start at 94°C for 5 minutes followed by 30 cycles of 94°C, 58°C, and 72°C each for 30 seconds, incubated at 72°C for 6 minutes, and held at 10°C. The reaction mix contained Ultrapure™ DNase/RNase-free distilled water, 1X Green GoTaq® Flexi Buffer, 1.5 mM $MgCl_2$, 0.2 mM GeneAmp dNTP mix (ABI, Carlsbad, CA, USA), 0.24 µM MCP1 F20, 0.24 µM MCP1 R320, 0.5 U GoTaq® HS DNA polymerase (Promega, Madison, WI, USA), and 1X FL07 liver cDNA. Purified PCR product was sequenced at the Atlantic Research Centre for Agricultural Genomics for sequencing where samples were processed using a 3130 Genetic analyzer (ABI, Carlsbad, CA, USA). Sequence obtained for MCP-1 was submitted to GenBank, accession number HQ163895 (Table 3).

4.2.3.2 Tumour necrosis factor alpha

Published mink mRNA sequence was available in GenBank for TNF-α accession number GU327784.

4.2.4 Standards

Copy RNA standards were created by designing T7 labeled primers with a T7 promoter sequence at the 5'-end from target specific sequences and running PCR followed by *in vitro* transcription, RNA purification, and reverse transcription.

4.2.4.1 T7 Promoter labeled DNA fragment

A T7 promoter labeled DNA fragment was produced by designing T7/dT labeled primers. Primers were designed using Primer 3 with forward primers modified with the 20 nucleotide T7 promotor sequence TAATACGACTCACTATAGGG attached to the 5'-end, while the reverse primer were modified by having a 15 nucleotide dT oligo attached to the 5'-end. A 48-68°C gradient PCR was run with the Dyad® Peltier Thermal Cycler (Bio-Rad, Carlsbad, CA, USA) and a 2% agarose gel electrophoresis was run to confirm the presence, size, and specificity of the PCR product. PCR product was then column purified or gel extracted, and finally quantified via spectrophotometer to determine DNA purity.

4.2.4.1.1 Monocyte chemoattractant protein-1

T7 PCR product was created using the primers MCP1 T7 F2 and MCP1 dt R280 (Table 2). PCR run conditions consisted of a hot start at 94°C for 5 minutes followed by 30 cycles of 94°C, 60°C, and 72°C each for 30 seconds, incubation at 72°C for 6 minutes, and a 10°C holding cycle. Reagents used were Ultrapure™ DNase/RNase-free distilled water, 1X PCR buffer containing 200 mM Tris-HCl (pH 8.4) and 500 mM KCl, 1.5 mM $MgCl_2$, 0.2 mM GeneAmp dNTP mix, 0.24 μM MCP1 T7 F72, 0.24 μM MCP1 dt R280,

0.5 U GoTaq® HS DNA polymerase (Promega, Madison, WI, USA), and 2X FL07 mink liver cDNA. PCR product was then gel extracted via the MiniElute gel extraction kit (QIAgen, Valencia, CA, USA) as per manufacturer's protocols with the exception that the 2% agarose gel was prepared with 0.085g of guanosine to protect DNA from ultra-violet degradation (Sigma® Life Science, St. Louis, MI, USA). Purified PCR product was quantified using the NanoDrop 1000 spectrophotometer (Fisher Scientific, Mississauga, ON, CAN).

4.2.4.1.2 Tumour necrosis factor alpha

T7 PCR was performed with primers T7 F40 and dt R419 using a 48-68°C gradient with run parameters identical to the sequence testing primers F89 and R309 (Table 2). A 2% agarose gel electrophoresis was run to confirm presence, size, and specificity of the PCR product resulting in 58°C being the optimal annealing temperature. The PCR product was then subsequently utilized as the cDNA for the re-amplification of the same primers above with the same conditions. The re-amplified PCR product was then pooled and gel extracted using the Wizard® SV Gel and PCR Clean-Up System (Promega, Madison, WI, USA) as per manufacturer's instructions to remove non-specific contaminants. Purified PCR product was quantified using the NanoDrop 1000 spectrophotometer (Fisher Scientific, Mississauga, ON, CAN).

4.2.4.2 Copy RNA

Molecular weight of the T7 promoter labeled sequence was calculated using Oligo Calc: Oligonucleotide Properties Calculator version 3.26 (last modified by WA

Kibbe 07/15/2010) in order to determine the amount of DNA to use to create a 100nM final concentration in a reaction volume of 8 µl. *In vitro* transcription was run using the MEGAshortscript Kit (ABI, Carlsbad, CA, USA) according to manufacturers instructions followed by RNeasy RNA purification with DNAse I treatment. The reaction contained 1X Reaction Buffer, 1X T7 Enzyme Mix, 7.5mM each ATP, CTP, GTP, and UTP, and 100nM template DNA. The mix was then incubated in the Dyad® Peltier Thermal Cycler for 4 hours at 37°C. A 0.7% agarose gel electrophoresis confirmed the quality and size of the purified copy RNA product, while the NanoDrop spectrophotometer was used to confirm quantity.

4.2.4.3 Single stranded DNA

Copy RNA was reverse transcribed using a High Capacity cDNA Reverse Transcription Kit using 1.0µg of copy RNA in a reaction volume of 20µl (ABI, Carlsbad, CA, USA) using the MultiScribe™ Reverse Transcriptase, by the same procedure used to create sample cDNAs **(**see section 4.2.2).

4.2.5 Quantitative real time polymerase chain reaction

Real time assays were assembled using the epMotion 5070 liquid handling robot (Eppendorf, Mississauga, ON, CAN) and quantified by the LightCycler® 480 Real-Time PCR System ll (Roche Applied Science, Laval, QUE, CAN). All samples were run on a single 384-well plate (Roche Applied Science, Laval, QUE, CAN) to remove plate-to-plate variation with triplicate technical replicates to reduce sampling error. Real time assays were run with a 9-point standard curve, which consisted of a 5-fold dilution series

of the copy RNA standards. The highest concentration standard consisted of $3.23X10^8$ copies for MCP-1 and $2.00X10^8$ copies for TNF-α. Melt curves were examined to eliminate the possibility of undetected false positives by ensuring that all samples and standards had consistent melting peaks indicating amplification of a single gene product (Figure 1).

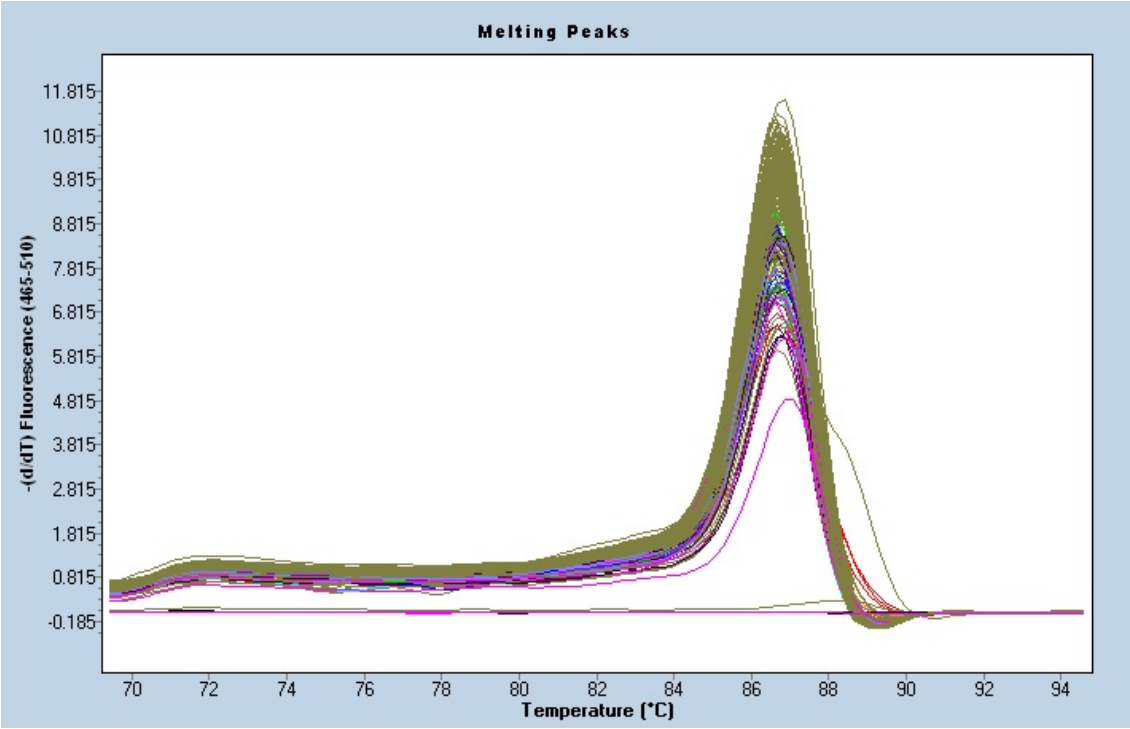

Figure. 1. Melt curve for TNF-α as an example of the amplification of a single gene product in real-time.

4.2.5.1 Real time primer design

Real time primers were designed from the appropriate mink (*Neovison vison*) mRNA sequences using Primer 3 to give an amplicon of 75-150 base pairs (Table 2). Primers were designed across exons attained from homologous human genes to minimize non-specific amplification. Real time primers were tested by running a 55-65°C gradient using the iQ^{TM}5 Real-Time PCR Detection System (Bio-Rad, CA, USA) to determine optimal annealing temperature and primer specificity. Primer pairs resulting in the highest efficiency and sensitivity (as shown by the lowest threshold cycles or quantification cycle for a given concentration) were selected as real time primers for the assay. Primers F149 and R266 resulted in the highest efficiency for MCP-1, while having the lowest cycle threshold at 60.0°C. For TNF-α F81 and R199 run at 62°C proved to be the most efficient (Table 2).

4.2.5.2 Plate preparation

The liquid handling robot completed all pipetting, thus reagents were prepared in stock solutions consisting of a mastermix, standards, samples, water, and Tris-Cl. A real-time mastermix was assembled in an Eppendorf epMotion 5075 mastermix reservoir consisting of Ultrapure^{TM} DNase/RNase-free distilled water, 1X PCR buffer containing 200 mM Tris-HCl (pH 8.4) and 500 mM KCl, 2.5 mM $MgCl_2$, 0.2 mM GeneAmp dNTP mix, 0.4 μM forward primer, 0.4 μM reverse primer, 0.8 U GoTaq® HS DNA Polymerase (Promega, Madison, WI, USA), and 1X Evagreen® (Biotium, Hayward, CA, USA). Forty-five (45)μl of mastermix was pipetted into a 96-well plate followed by 5μl of each sample cDNA or 5μl of DNase/RNase-free distilled water for the blank, and

mixed twice by pipetting. Ten (10)µl of each mixture was then pipetted onto the 384-well plate in triplicate. Standards were prepared by adding 90µl of 10mM Tris-Cl pH 7.4 to 10µl of a 0.01X concentration of copy RNA standard and was aliquoted into a 1.5ml centrifuge tube. 10mM of Tris-Cl, pH 7.4 was aliquoted into a 1.5ml centrifuge tube, from which the liquid handling robot pipetted 80µl of the Tris-Cl into 9 wells on a 96-well plate. Sixty (60)µl of the stock standard was pipetted onto the 96-well plate, from which subsequently 20µl was mixed continually into the next well containing 80µl of Tris-Cl until a 5-fold dilutions series was created. Five (5)µl of each standard was then mixed with 45µl mastermix and 10µl was aliquoted onto the 384-well plate in triplicate as for the samples and blanks, above. The plate with all components loaded was run on the LightCycler® LC 480 II (Eppendorf, Mississauga, ON, CAN).

4.2.5.3 Reaction conditions and parameters

Run conditions for both MCP-1 and TNF-α were identical with the exception of the annealing temperature. Real-time PCR parameters consisted of a hot start at 94°C for 2 minutes followed by 45 cycles of 94°C, 60°C for MCP-1 or 62°C for TNF-α, and 72°C in sequence each held for 30 seconds. This was followed by a melt curve containing premelt at 95°C for 10 seconds, 65°C 1 minute, 70°C for 1 second, followed by a melt curve from 70°C to 95°C where 5 acquisitions were taken with an increasing temperature gradient of 1°C, and held at 20°C for 1 second.

4.2.6 Data normalization

The reference gene used to normalize both MCP-1 and TNF-α was glyceraldehyde-3-phosphate dehydrogenase (GAPDH) (Pal 2011). GAPDH was chosen as the internal standard since the gene has been demonstrated to possess a constant level of gene expression among all cells in liver tissue enabling correction for experimental variation (Lisowski *et al*. 2008; Xu *et al*. 2011). The real-time assay was prepared identically to both MCP-1 and TNF-α using the liquid handling robot. The mastermix contained: Ultrapure™ DNase/RNase-free distilled water, 1X PCR buffer, 2.5 mM $MgCl_2$, 0.2 mM GeneAmp dNTP mix, 0.4 μM forward primer, 0.4 μM reverse primer, 0.8 U GoTaq DNA polymerase, and 1X Evagreen® (Biotium, Hayward, CA, USA). Real-time PCR parameters consisted of a hot start at 95°C for 2 minutes followed by 40 cycles of 95°C for 10 seconds, 61°C for 20 seconds, and 72°C for 30 seconds. This was followed by a melt curve containing premelt at 95°C for 10 seconds, 65°C 1 minute, 70°C for 1 second, followed by a melt curve from 70°C to 95°C where 5 acquisitions were taken with an increasing temperature gradient of 1°C, and held at 20°C for 1 second. Ratios were calculated by dividing the concentration of each gene (calculated as the geometric mean of the triplicate samples, by the LightCycler® LC 480 II software) by the reference gene resulting in a normalized gene expression ratio.

Table 1. GenBank sequences where regions with the largest homology were used to design primers for mink (*Neovison vison*) MCP-1 sequence testing.

Species	**GenBank accession number**
Ferret (*Mustela putorius*)	EZ_470131
Ferret (*Mustela putorius*)	EZ_509795
Cat (*Felis catus*)	DQ_835566
Dog (*Canis lupus familiaris)*	NM_001003297
Humans (*Homo sapiens*)	NM_002982
Horse (*Equus caballus*)	EU438774
Pig (*Sus scrofa*)	NM_214214

Table 2. Mink (*Neovison vison*) GAPDH, MCP-1, and TNF-α primer pairs designed from homologous sequences using the software Primer 3. A, B: Primers used to amplify mink specific MCP-1 for sequencing. C, D: T7 promoter labeled primers for *in vitro* transcription producing copy RNA. E, F, G: Real time primers for the qRT-PCR assay.

Target	**Primer Pairs**	**Forward primer**	**Reverse primer**	**GenBank accession numbers**
A) *MCP-1*	F89/R309	5'-tctccagtcacctgctgcta-3'	5'-attcatggctttgcagtttg-3'	Refer to Table 1
B) *MCP-1*	F20/R320	5'-ctcctctgcctgctgctc-3'	5'-tcagagtgagtattcatggcttt-3'	Refer to Table 1
C) *MCP-1*	T7 F2/dt R280	5'- taatacgactcactataggg ctcctctgcctgctgctc-3'	5'-ttttttttttt gcagtttggttctgggttt-3'	HQ_163895
D) *TNF-α*	T7 F40/dt R419	5'-taatacgactcactataggg ggcccagacagtcaaatcat-3'	5'-tttttttttt tagacccctcccaggtagatg-3'	GU_327784
E) *MCP-1*	F149/R266	5'-agcagcaagtgtcccaaag-3'	5'-gggttttctt-gtccaggtgt-3'	HQ_163895
F) *TNF-α*	F81/R199	5'-agcctgtagctcatgttgt-3'	5'-cactattagctggttgtctgt-3'	GU_327784
G) *GAPDH*	F36/R119	5'-aatgcctcctgtaccaccaa-3'	5'-ggtcatgagtccctccacaa-3'	AF_076283 Pal 2011 Rouvinen-Watt *et al.* 2012

Table 3. Mink (*Neovison vison*) nucleotide and amino acid sequence for MCP-1 submitted to GenBank.

Target	**Nucleotide sequence (5'- 3')**	**GenBank accession number**
MCP-1	tctcctctgcctgctgctcaccgccgctgccatcagcatccaggtgctcgc ccagccagatgcaattaattctccagtcacctgctgctacacattcaccaat aagaagatctcagtgcagaggctgacgagctataagagagtcaccagca gcaagtgtcccaaagaagctgtgatcctcaagacattccttaacaaggaga tctgcgctgaccccagtcagaagtgggtccgggattccatggcacacctg gacaagaaaacccagaaccaaactgcaaagcca	HQ163895
MCP-1	LLCLLLTAAAISIQVLAQPDAINSPVTCCYTFTN KKISVQRLTSYKRVTSSKCPKEAVILKTFLNKEI CADPSQKWVRDSMAHLDKKTQNQTAKP	ADM87307

4.3 Bile duct histological quantification

Hematoxylin and eosin stained slides were used to determine the quantity of bile ducts present in the portal triads of each treatment. One slide per sample was randomly coded indicating that observations were blind to both treatment and sex of the mink. Slides were analyzed using a digital imagining system containing a light microscope (Leica DM500, Leica Microsystems Ltd., Switzerland) with a digital colour microscope camera (Leica Application Suite EZ, LAS EZ, Leica Microsystems). Each slide had two liver slices present and the slice with the least amount of artifacts and best clarity was chosen for analysis. Slides were divided into four equal quadrants by using the stage micrometer. Slides were scanned with the 10x objective and one portal triad was chosen per quadrant to be imaged at 400X magnification. Portal triads were chosen based on the criteria that portal triads must have a hepatic artery, hepatic vein, and bile ducts present, fit into one 40x focal view, and have no artifacts present. Photos were analyzed using Image Pro Plus 7.0 software (Media Cybernetics, Bethesda, MD, USA) and were processed using a high Gaussian resolution and/or sharpening when required. Bile ducts were counted on each photo and manual tags were saved. Bile ducts were tagged based on the characteristics that the duct possessed cuboidal shaped epithelium with a visible lumen (Demetris *et al*. 1996; Ross and Pawlina 2006).

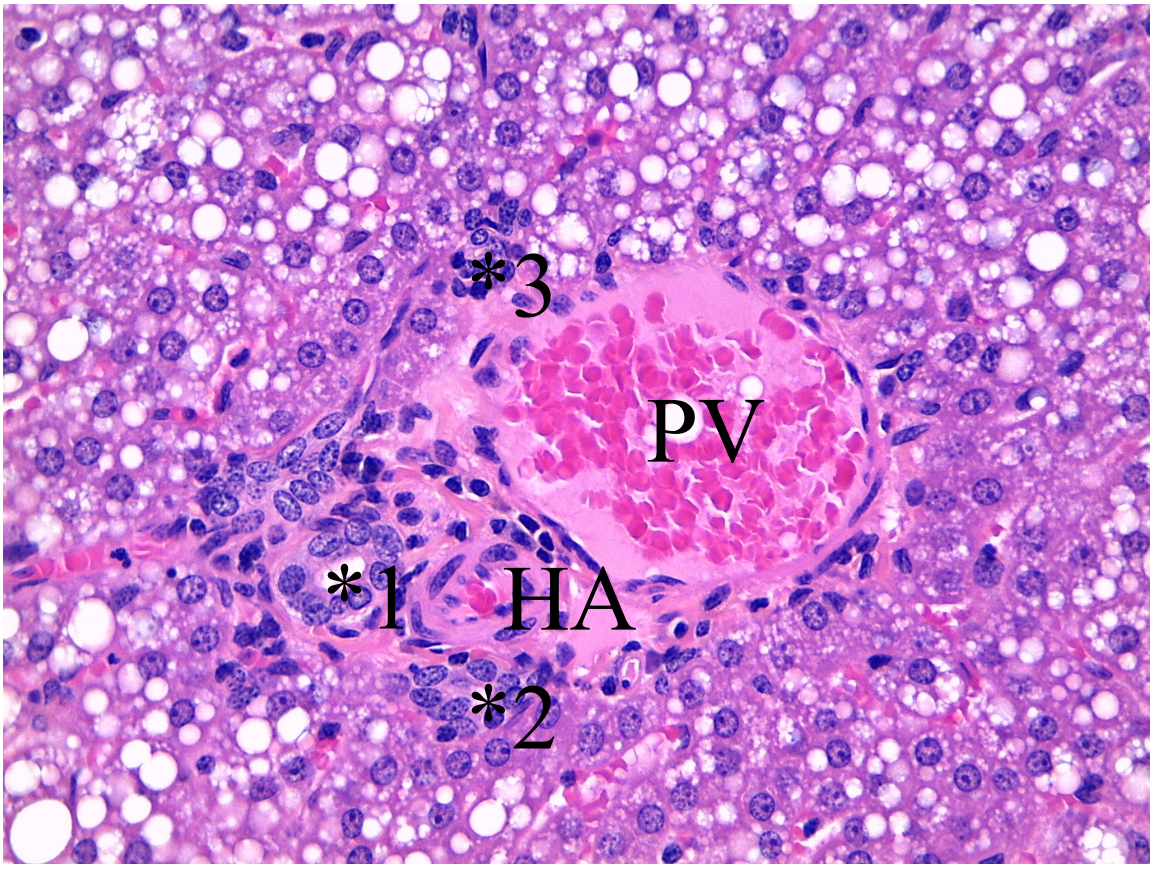

Figure 2. Portal triad of a female fasted for five days containing a portal vein (PV), hepatic artery (HA), and bile ducts. Black asterisks indicate presence of a bile duct with corresponding numbers. The image represents one focal view at 40X magnification.

4.4 Statistical Analyses

The experimental design used was 2 × 6 factorial with two sexes and six treatment groups. The data were analyzed using Proc Mixed in SAS version 9.2 (SAS Institute Inc., Cary, NC, USA) to examine the effects of the sex and the fasting regimes and their interaction on the measured variables. A Pearson's correlation coefficient was calculated between the response variables using SAS version 9.2, while a linear regression analysis was performed to examine the relationship between the mRNA expression levels. Log transformations were performed on MCP-1, TNF-α, and average bile duct data to achieve normality. Graphs represent back-transformed data with transformed p-values and statistical significance was set at P= 0.05. The results are presented as lsmeans ± standard error of the mean (SEM).

CHAPTER 5.0 RESULTS

5.1 Glyceraldehyde-3-phosphate dehydrogenase mRNA levels

Normalizing gene GAPDH had no significant treatment, sex, or interaction effect (P= 0.124; P= 0.446; P= 0.343; Pal 2011).

5.2 Tumour necrosis factor alpha mRNA levels

The TNF-α qRT-PCR assay had an efficiency of 1.95 with a R^2= 0.993. Coefficient of variation for the assay was 18.17%. For TNF-α, fasting mink for 1-7 days and RF resulted in a significant treatment effect, while no sex effect or interaction effects between treatment and sex were observed (Table 4). Normalized liver mRNA expression of TNF-α was the highest in male and female mink fasted for 5 days, although there was no significant difference from mink fasted for 7 days. Fasting for 5 days resulted in greater than 1.5-fold difference from 0, 1, and 3 treatments, while having a greater than 4.5-fold difference from the RF treatment. Similar effects were found with 7 days resulting in a greater than 1.5-fold difference from 0, 1, and 3 days, while having a greater than 4-fold difference from mink in the RF treatment. The lowest expression of TNF-α was the mink in the RF treatment. There was no significant difference between in the 0, 1, 3, and RF treatments.

Table 4. P-values for analysis of TNF-α liver mRNA expression levels normalized to GAPDH in mink fasted 0, 1, 3, 5, or 7 days or fasted for 7 days followed by a period of re-feeding of 28 days. $P<0.05$ indicates statistical significance.

Effect	**P-value**
Treatment	**0.029**
Sex	0.127
Interaction	0.168

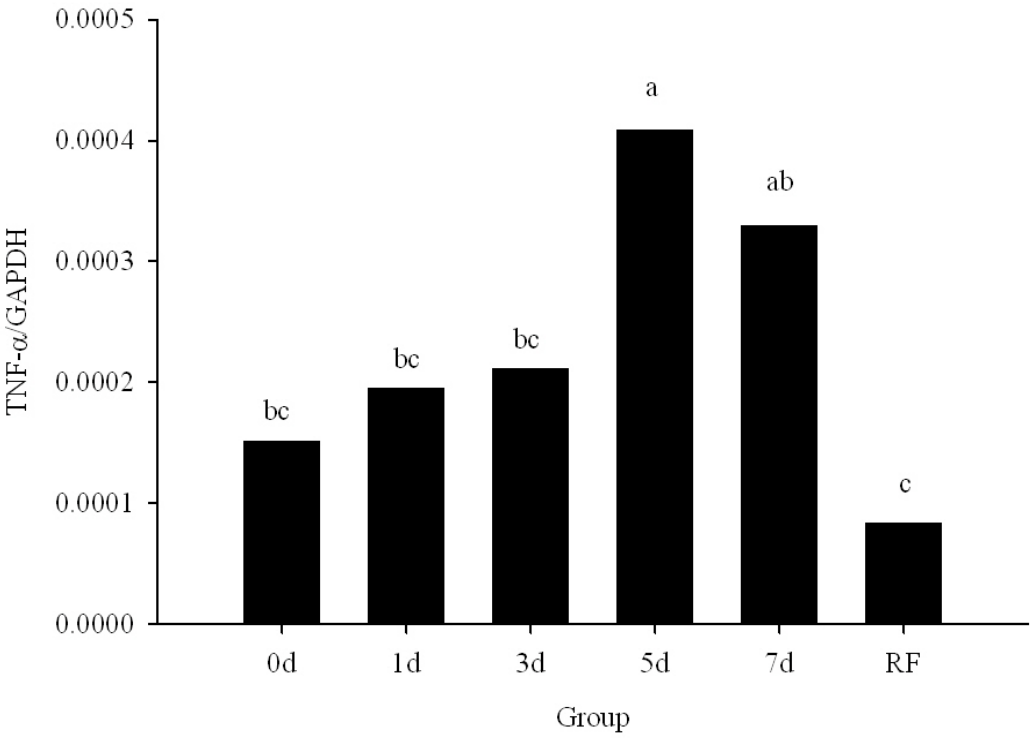

Figure 3. Effect of fasting on liver TNF-α/GAPDH mRNA expression ratio in mink fasted 0, 1, 3, 5, or 7 days or fasted for 7 days followed by a period of re-feeding of 28 days. Differing letters indicate significant differences between groups ($P<0.05$).

5.3 Monocyte chemoattractant protein-1 mRNA levels

The MCP-1 qRT-PCR assay had an efficiency of 1.94 with R^2= 0.997 and all samples peaking within the standard curve. Coefficient of variation for the assay was 9.6%. The MCP-1 assay resulted in a significant treatment effect, while having no sex effect or interaction effect (Table 5). Mink fasted for 7 days resulted in the highest liver mRNA expression of MCP-1; however not significantly different from mink fasted for 5 days. Fasting for 5 and 7 days resulted in a greater than 2.5-fold difference from treatments 0, 1, and 3, while having a greater than 4.5-fold difference from the RF treatment. The lowest expression of MCP-1 was present in mink in the RF treatment.

Table 5. P-values for analysis of MCP-1 liver mRNA expression levels normalized to GAPDH in mink fasted 0, 1, 3, 5, or 7 days or fasted for 7 days followed by a period of re-feeding of 28 days. P<0.05 indicates statistical significance.

Effect	**P-value**
Treatment	**<0.001**
Sex	0.242
Interaction	0.339

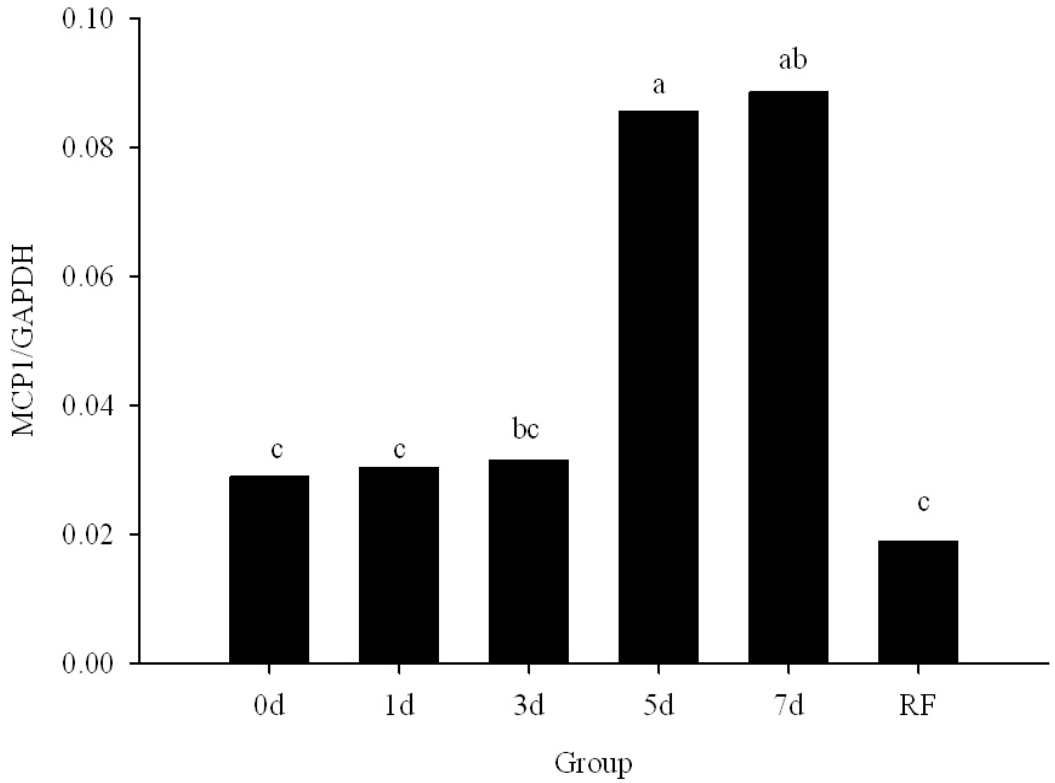

Figure 4. Effect of fasting on liver MCP1/GAPDH mRNA expression ratio in mink fasted 0, 1, 3, 5, or 7 days or fasted for 7 days followed by a period of re-feeding of 28 days. Differing letters indicate significant differences between groups ($P<0.05$).

5.4 Bile duct quantification

Histological evaluation of the number of bile ducts per foci revealed that there was no significant treatment, sex, or interaction effect observed (Table 6). Male mink fasted for 5 days had the highest average of bile ducts with 2.30±0.215 per field of view, while female mink fasted for 7 days had the lowest with 1.50±0.196 per field of view (Table 7).

Table 6. P-values for analysis of bile duct numbers per field of view in mink fasted 0, 1, 3, 5, or 7 days or fasted for 7 days followed by a period of re-feeding of 28 days. $P<0.05$ indicates statistical significance.

Effect	**P-value**
Treatment	0.754
Sex	0.200
Interaction	0.221

Table 7. Average number of bile ducts present per focal view of mink fasted 0, 1, 3, 5, 7 days or fasted for 7 days followed by a period of re-feeding of 28 days, standard error of means in parentheses.

Treatment	**Average number of bile ducts**	
	Male (SEM)	Female (SEM)
0	1.85 (0.215)	2.00 (0.215)
1	1.80 (0.215)	1.90 (0.215)
3	1.70 (0.215)	2.00 (0.215)
5	2.30 (0.215)	1.70 (0.215)
7	1.90 (0.215)	1.50 (0.196)
RF	2.20 (0.215)	1.80 (0.240)

5.5 Correlations between response variables

Comparison of liver mRNA expression levels of TNF-α and MCP-1 resulted in a significant correlation (Table 8). TNF-α was also strongly correlated with liver fat percent, while MCP-1 was only marginally correlated (Table 8). A significant linear relationship was present between MCP-1 and TNF-α as follows MCP-1/GAPDH = 0.0138 + 147.237 × (TNF-α/GAPDH), R^2= 0.475, P< 0.001 (Figure 5).

Table 8. Correlation of TNF-α and MCP-1 normalized to GAPDH with each other and with liver weight, liver fat percent, and number of bile ducts per field of view.

Variables	**Correlation coefficient, r**	**P-value**
TNF-α/GAPDH vs. MCP-1/GAPDH	**0.689**	**<0.001**
TNF-α/GAPDH vs. liver weight	0.209	0.108
TNF-α/GAPDH vs. liver fat percent	**0.478**	**<0.001**
TNF-α/GAPDH vs. avg. no. bile ducts	-0.044	0.738
MCP-1/GAPDH vs. liver weight	0.144	0.272
MCP-1/GAPDH vs. liver fat percent	0.223	0.086
MCP-1/GAPDH vs. avg. no. bile ducts	0.172	0.188

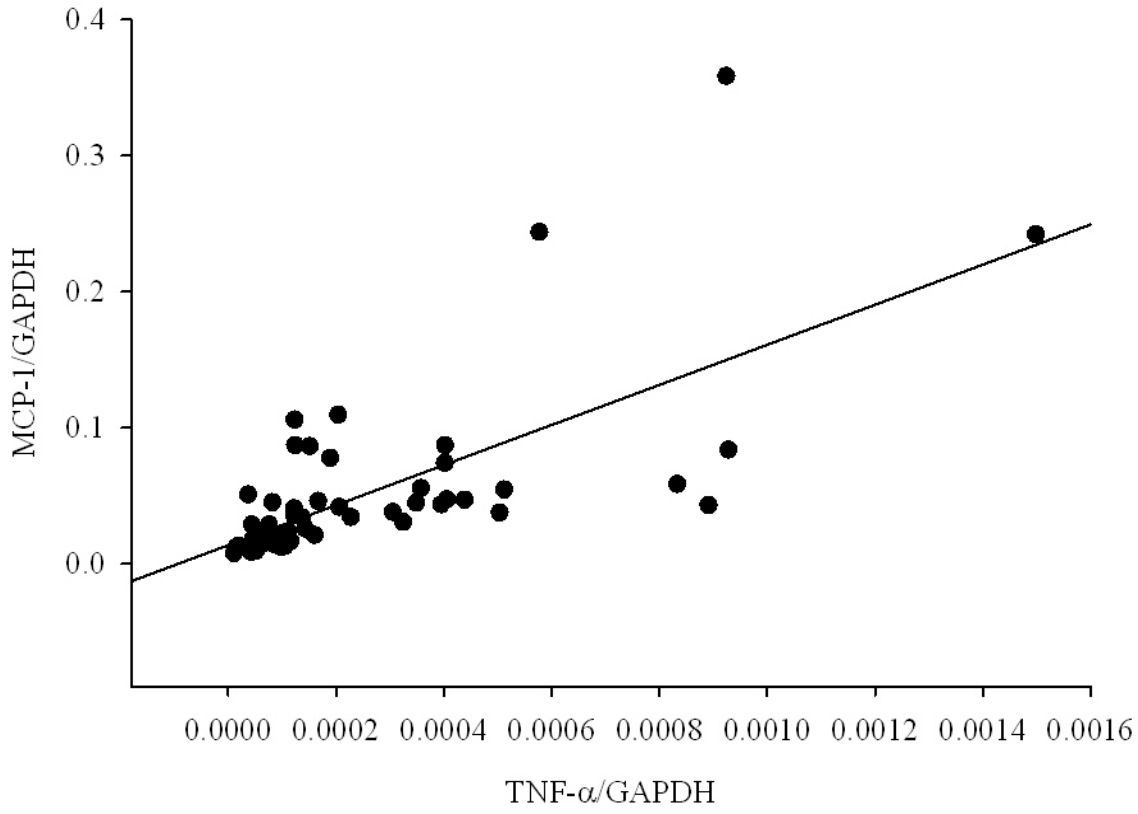

Figure 5. Linear regression demonstrating the relationship present between TNF-α and MCP-1 liver mRNA expression levels, MCP-1/GAPDH = 0.0138 + 147.237 × (TNF-α /GAPDH), R^2= 0.475, P< 0.001.

CHAPTER 6.0 DISCUSSION

6.1 Induction of hepatic steatosis in mink

Quantifying liver mRNA expression of the targets TNF-α and MCP-1 in a fasting model is innovative. Mink from the current study possessed a significantly lower body weight following 5 and 7 days of fasting, while 1 and 3 days did not differ from day 0 (Rouvinen-Watt *et al*. 2010). When considering liver lipid mass and liver lipid percentage there was a significant increase in mink fasted for 3-7 days in comparison to control animals (Rouvinen-Watt *et al*. 2010). In the mink fasted for 0 and 1 days the liver fat percent was on average 6%, while in the mink fasted for 3 days it increased to above 13%. Prolonged fasting for 5 and 7 days resulted in the highest liver fat percentages of 19.0 and 19.7%, while the mink in the RF treatment had the lowest liver fat content of 5.3%. Previous studies by Clausen (1992), Bjornvad *et al.* (2004) and Mustonen *et al.* (2005) have documented the effects of fasting in mink on liver weight and lipid content, which support our current findings of mink fasted for 1-7 days. In cats, Biourge *et al.* (1994) discovered that hepatic lipidosis was observed in 12 of 15 cats after 5-7 weeks of fasting associated with a 30-35% decrease in total body weight. These studies are supported in humans where Moller *et al*. (2008) found that fasting of lean males for 36 hours resulted in an increase in intrahepatic lipid profiles measured via magnetic resonance spectroscopy (H-MRS). Furthermore, cases of anorexia nervosa have been reported with marked increases in liver weight and the development of steatosis (Sakada *et al.* 2006). The increased liver lipid profiles demonstrated in the preceding fasting models are similar to those of obese models (Fabbrini *et al*. 2010). Westerbacka and

associates (2005) found a positive correlation between dietary fat and liver lipid content in overweight non-diabetic women, while Pietiläinen *et al*. (2005) concluded that acquired obesity is associated with an increase in liver fat and insulin resistance independent of genetic factors. Kotronen and colleagues (2007) supported these results by concluding that obese patients with the metabolic syndrome had higher lipid profiles. In cats, development of FIHL has been demonstrated only in animals with a history of obesity (Blanchard *et al*. 2004). The collective effects of fasting and diet induced obesity render both approaches as ideal methods to induce fatty liver disease due to their significant association with liver lipid content.

6.2 Mink TNF-α mRNA liver expression

Our results show that fasting mink for 1-7 days and RF resulted in a significant treatment effect with mink fasted for 5 and 7 days having the highest liver mRNA expression of TNF-α. The role of TNF-α in the progression of NAFLD to NASH has been previously documented by several studies. In human models, Crespo *et al.* (2001), Guerra Ruiz *et al*. (2007), and Cayon *et al*. (2008) found that obese patients with NASH had a significant increase in liver mRNA expression of TNF-α when compared to obese control patients without NASH. Bertola *et al*. (2010) discovered a 4.6-fold difference in TNF-α mRNA expression when comparing obese NASH patients to obese patients with a histological scored diagnosis of steatosis. In mice, Park *et al.* (2010) demonstrated that obesity resulted in an elevation in mRNA and protein levels of TNF-α in normal livers and livers with hepatocellular carcinoma, while Endo *et al.* (2007) were able to stimulate an increase in liver weight and hepatic triglyceride levels by injecting human

recombinant TNF-α into fasted mice. A report by Lin *et al.* (2000) indicated that leptin deficient mice administered metformin reversed the effects of fatty liver disease by a method that involves inhibition of hepatic expression of TNF-α and TNF-inducible factors that promote hepatic lipid accumulation. Hepatic expression of TNF-α has also been demonstrated to be increased in alcohol-induced fatty liver disease (ALD), which resembles the development of obesity and fasting induced hepatic steatosis (Iimuro *et al* 1997, Lin *et al*. 1998). A study by Yin and associates (1999) discovered that TNF-receptor-deficient mice were completely protected from developing steatohepatitis induced by alcohol. Diethl (2001) found that TNF-α was incapable of inducing fatty liver disease in diabetic mice leading to the conclusion that TNF-α is not the sole stimulant that triggers the development of fatty liver. In the mink from the current study, Pal (2011) found based on liver NAI scores that after the fifth day of fasting the mink had an increase from mild to moderate fatty liver. The increase in NAI scores was shown to occur at the same time point when an increase in liver TNF-α mRNA expression levels was established. This indicates that mink liver TNF-α mRNA levels may respond to fasting similarly to the other species mentioned above. These studies support the conclusion that liver TNF-α mRNA expression levels have a positive relationship with hepatic steatosis and its progression to NASH, whether it be stimulated by fasting, obesity, or alcohol.

Several studies have demonstrated the relationship between TNF-α and the development of fatty liver, but the pathological mechanisms remain unclear. TNF-α is an inflammatory cytokine that has the capability of hindering lipid and glucose metabolism,

which both promote the development of fatty liver (Popa *et al.* 2007). Fatty liver develops when the uptake and synthesis of FA occurs at a rate faster than the oxidation and secretion from the liver, which is associated with the development of insulin resistance (Fabbrini *et al*. 2010). TNF-α induces insulin resistance by interfering with insulin signaling mainly through a serine-phosphorylation and a tyrosine-dephosphorylation of the insulin receptor susbstrate-1 (IRS-1) causing inactivation and degradation of the receptor (Matsuzawa 2005; Capurso and Capurso 2012). TNF-α further promotes insulin resistance by reducing glucose transporter 4 (Glut-4) expression in peripheral tissue resulting in a decreased glucose transport and attenuating adiponectin expression (Trayhurn and Wood 2005; Tessari *et al*. 2009). The inhibition of insulin signaling results in increased lipolysis, glycogenolysis, and gluconeogenesis in the liver increasing circulating levels of glucose and FFA (Savage *et al*. 2007). TNF-α facilitates the development of fatty liver by increasing production of FFA from both adipose tissue and liver by lipolysis and increasing *de novo* FA synthesis by increasing levels of hepatic citrate leading to hypertriglyceridemia (Hotamisligil *et al.*1995; Chen *et al.* 2009; Yoshida *et al.* 2010). In the same mink from this study, ACC-1 and FAS liver mRNA expression levels increased in response to fasting suggesting that hepatic DNL further promotes the development of fatty liver by increasing the availability of MUFA for storage (Rouvinen-Watt *et al*. 2012). TNF-α furthermore affects the oxidation and secretion of FFA by diminishing clearance of VLDL from the liver, stimulating over production of VLDL, decreasing expression of apoE in hepatocytes resulting in TAG rich lipoproteins remaining in circulation for a longer period of time, and altering the phenotypic state of pre-adipocytes resulting in the inability to store lipids properly (Popa

et al. 2007; Qin *et al*. 2008; Isakson *et al*. 2009). Given the role that TNF-α plays in lipid and glucose metabolism TNF-α may be responsible for the increase in the NAI score enhancing disease progression, although further research is required to confirm this.

Obesity and inflammation are highly integrated processes in the pathogenesis of insulin resistance, diabetes, dyslipidemia, and NAFLD. Simple steatosis is defined by the accumulation of TAG in liver cells accounting for greater than five percent of total liver weight (Brunt *et al.* 2009). In our study we found that TNF-α liver mRNA expression levels had a strong correlation with liver fat percent, which is a novel finding. In subjects with the metabolic syndrome, which shares many pathological similarities to NAFLD, liver fat content was significantly increased when compared to those subjects without the syndrome, independent of age, gender, and body mass index (Kotronen *et al*. 2007). In mice, dosing with TNF-α resulted in an increase in liver weight and hepatic TG levels including in a fasted state (Endo *et al*. 2007). Supporting this conclusion a previous study showed that TNF-α induced an increase in hepatic TG production, causing hyperlipidemia in mice (Feingold *et al*. 1989). Our study is the first to document the correlation between TNF-α liver mRNA expression and liver fat percent in mink, which further demonstrates the potential involvement of inflammation in the excessive accumulation of lipids in the liver and the development of hepatic lipidosis.

6.3 Mink MCP-1 mRNA liver expression

MCP-1 is a chemokine that has been implicated in the transition from simple steatosis to steatohepatitis by recruiting macrophages to liver tissues. Our data suggests

that mink liver mRNA expression levels are positively associated with period of fasting since mink fasted for 5 and 7 days were significantly different from those fasted for 0, 1, 3, and re-fed treatments. Several studies have documented the involvement of MCP-1 in the development of liver inflammation in various fatty liver models. In morbidly obese patients, Bertola and associates (2010) found that those patients with NASH had a higher mRNA expression of MCP-1 when compared to controls. Using $LDLr^{-/-}$ mice as an animal model of high-fat, high-cholesterol diet-induced liver steatosis Rull *et al*. (2009) found that the rapid dietary induction of hepatic mRNA MCP-1 expression was paralleled by a simultaneous increase in plasma MCP-1 that was strongly associated with the degree of liver steatosis. In a similar study using apolipoprotein E-deficient mice that develop atherosclerosis and steatohepatitis in response to high-fat and cholesterol diets resulted in an increased liver expression of MCP-1 (Tous *et al*. 2006). These results were supported by another mouse model where steatosis was induced using a diet devoid of methionine and choline (MCD) leading to an increase in the hepatic expression levels of MCP-1 mRNA (Luyendyk *et al*. 2010). Kassel *et al*. (2010) built on the MCD model by concluding a MCP-1 deficiency did not impact liver steatosis or inflammation in mice fed the MCD diet. However, MCP-1-deficiency reduced profibrogenic gene expression and liver fibrosis in this model. In alcohol-induced models of fatty liver, Bautista (1998), Maher (2008), and Nanji *et al.* (2001) have shown that MCP-1 is up regulated in the presence of alcohol-induced necroinflammatory changes in the liver in rats. In humans with alcoholic hepatitis, Degré and associates (2012) found that patients demonstrated significantly higher hepatic MCP-1 mRNA expression levels than control subjects, which was correlated with disease severity and neutrophil infiltrates. The collective effects

demonstrated by the use of several different animal models strengthen the conclusion that MCP-1 is involved in liver inflammation associated with the development of steatohepatitis whether it be diet, alcohol, or fasting induced.

The infiltration of macrophages into liver tissue is a critical contributing factor in the development of chronic inflammation and the development of NASH, which is regulated by the expression of both MCP-1 and its corresponding receptor CCR2 present on endothelial cells, macrophages, Kupffer cells, and HSC (Obstfeld *et al*. 2010). Hepatic macrophages are classified into two populations, resident Kupffer cells and recruited macrophages (Miura *et al*. 2012). These populations can be divided into two phenotypes being M1 pro-inflammatory macrophages and M2 anti-inflammatory macrophages (Mantovani *et al.* 2004). Miura and associates report that macrophages of wild-type (WT) mice with steatosis induced by a choline-deficient amino acid-defined (CDAA) diet expressed high levels of TNF-α and MCP-1, but cells of $CCR2^{-/-}$ mice do not. This indicates that recruited macrophages are M1 pro-inflammatory, while Kupffer cells are less inflammatory with a lower CCR2 expression. These results are supported by Obstfeld and associates (2010) where recruited bone-marrow derived macrophages possessed a higher expression of CCR2 and the M1 inflammatory phenotype than Kupffer cells. In genetically obese db/db mice, Tamura *et al*. (2008) found that a pharmacologic antagonist of CCR2 reduced hepatic steatosis. In two *in vivo* models, Baeck and colleagues (2012) found that administering the CCR2 inhibitor mNOX-E36 to mice effectively inhibited monocyte chemotaxis to the liver. These results were further supported by using the inhibitor on CCl_4 and MCD diet-induced mice models

significantly reduced the infiltration of macrophages into the liver, decreased the hepatic expression of TNF-α, and a lower level of fatty liver degeneration leading to ameliorated hepatic steatosis was detected in mice treated with mNOX-E36 (Baeck *et al*. 2012). The reduced infiltration of pro-inflammatory macrophages into liver tissue and the consequent amelioration of steatosis further demonstrate the importance of MCP-1 and CCR2 in the progression of chronic inflammation and the development of NASH.

Excess hepatic fat accumulation occurs when the homeostasis of FFA β-oxidation, exportation by lipoproteins, or storage by esterification is disrupted (Feldstein *et al.* 2004). Liver MCP-1 mRNA expression showed a marginally significant correlation to liver fat percent. This increase in liver expression of MCP-1 indicates a marked change in liver structure. Greco *et al.* (2008) analyzed the livers of NAFLD patients containing a high liver fat percentage and controls with a low liver fat percentage by qRT-PCR and microarray analysis. Their results showed a significant correlation between liver fat and MCP-1 liver mRNA and gene expression. These findings were supported by Westerbacka *et al.* (2008) who used patients with varying liver fat percentages ranging from normal to NAFLD and found that there was a positive correlation between liver fat percent and MCP-1 liver mRNA expression measured via qRT-PCR. In C57BL/6 male mice, Stanton *et al.* (2011) discovered a high fat diet resulted in significant increases in liver mRNA expression for MCP-1 levels at 16 and 26 weeks on the diet. In obese mice, an absence of the C-C motif chemokine receptor-2 protected the liver against an accumulation of lipids (Weisberg *et al.* 2006). These studies together indicate that liver fat accumulation is positively associated with liver MCP-1 mRNA levels subsequently leading to the

development of fatty liver disease.

6.4 Effect of re-alimentation on TNF-α and MCP-1 mRNA expression

The effect of re-feeding of fasted animals on the mRNA expression levels of TNF-α and MCP-1 has not been well documented. Our study showed that mink in the RF treatment had the lowest TNF-α and MCP-1 liver mRNA expression levels and returned to baseline levels since there was no significant difference from those mink fasted for 0, 1, and 3 days. A similar study was conducted by Straus and Takemoto (1990) measuring insulin-like growth factor-1 (IGF-1) liver mRNA from rats that were short-term fasted and re-fed for 24 hours finding that mRNA levels rebounded after fasting, but not to the initial control levels. Renier and associates (1996) demonstrated that there was a positive correlation between IGF-1 and TNF-α since IGF-1 is a monocyte/macrophage activating factor that enhances TNF-α production. A contrasting relationship has been demonstrated in rats fasted short-term for 8 hours and re-fed ad-libitum for 3 hours revealing that the liver expression levels of genes involved with FA oxidation, peroxisome proliferator activated receptor alpha (PPAR-α), and carnitine palmitoyltransferase 1a (CPT1) were significantly increased after 8 hours and returned to control levels after re-feeding (Palou *et al.* 2008). Kersten *et al.* (1999) support this relationship elucidating that PPAR-α mRNA levels increase in response to fasting to accommodate the increased demand for hepatic FA oxidation, a response that is shown in PPAR-α null mice who develop hepatic steatosis in response to fasting. In endothelial cells, PPAR-α has been demonstrated to elevate the expression levels of MCP-1 and TNF-α (Lee *et al*. 2000). The effect of fasting on the liver stimulates an increase in IGF-1 mRNA expression, which has a

negative association with the expression of PPAR-α and sterol regulatory element binding protein-1 (SREBP-1). Re-alimentation after fasting resulted in mRNA expression levels of IGF-1, PPAR-α, and SREBP-1 returning close to or lower than baseline levels. Given the relationship TNF-α and MCP-1 have with these proteins, one would expect that the mRNA expression would increase in response to fasting and returning to baseline levels in response to re-feeding, which supports the effect demonstrated when mink are re-fed after a period of fasting. TNF-α and MCP-1 liver mRNA expression levels returning to baseline after re-alimentation along with the moderate recovery of body weight, liver fat percent, and liver morphology indicates that inflammation can be diminished and homeostasis can be restored after a period of re-feeding (Rouvinen-Watt *et al.* 2010).

6.5 Correlation between TNF-α and MCP-1

Communication among cells is accomplished by the secretion and binding of proteins (O'Shea and Murray 2008). Cytokines and chemokines are released after a cell is triggered by a specific cue and may act in an autocrine, endocrine or a paracrine fashion (Coppack 2001). Fasting mink resulted in a strong correlation between TNF-α and MCP-1 liver mRNA expressions. This relationship is supported by Murao *et al*. (2000) indicating that TNF-α is capable of stimulating the release of MCP-1 from vascular endothelial cells. In human liver cells, incubation with TNF-α resulted in a 1.6-fold increase in the secretion of MCP-1 (Marra *et al*. 1993). Administration of LPS, TNF-α, or IL-1 to rats resulted in a hepatic increase in MCP-1 expression *in vivo* (Czaja *et al*. 1994). In male mice, Stanton *et al.* (2011) discovered significant increases in liver mRNA

expression for both MCP-1 and TNF-α levels at 16 and 26 weeks on a high fat diet. Given the ability of TNF-α to stimulate MCP-1 expression, and their demonstrated roles in the development of NAFLD and NASH, TNF-α and MCP-1 are both ideal candidates as biomarkers in the development of these liver diseases.

6.6 n-3/n-6 fatty acid ratios

The development of nursing sickness and the subsequent hepatic lipidosis has been implicated with an unfavorable n-3/n-6 PUFA ratio similar to that of humans with NAFLD and the metabolic syndrome (Rouvinen-Watt *et al.* 2010). Food deprivation has been associated with mobilized fat stores that favor the depletion of n-3 PUFA leading to an increase in FA and TAG synthesis increasing liver lipid accumulation (Mustonen *et al*. 2009, Nieminen *et al.* 2009). In the mink in our study, fasting for 1-7 days resulted in significantly lower n-3 PUFA proportions in liver tissues (Rouvinen-Watt *et al*. 2010) and is supported by studies on fasting in the American marten and raccoon dog (Mustonen *et al.* 2007, Nieminen *et al*. 2006). An increase in FA in the cell membranes of hepatocytes results in an increase in the synthesis of pro-inflammatory eicosanoids in the liver. Rapid fluctuations in liver n-3/n-6 PUFA ratios may be a contributing trigger to the inflammatory response demonstrated in our study explaining the significant correlation in liver mRNA expression of TNF-α and MCP-1.

6.7 Bile duct proliferation

Fasting mink had no significant effect on the bile duct proliferation and did not result in any difference in the quantity of bile ducts present per foci. The quantity of bile

ducts has been implicated as having a positive relationship with the progression of disease severity in NAFLD which our results do not support (Sasaki *et al*. 2010; Chiba *et al*. 2011). In bonnet monkeys with NAFLD Nagarajan and associates (2008) reported a ductular reaction/proliferation as indicated by newly formed bile ducts in the portal area surrounded by fibrosis. Our study involved the quantification of bile ducts present within one field of view and all of those portal triads that didn't fit were omitted. There is a possibility that omitting larger portal triads limits the variability demonstrated and thus future studies would focus on imaging the entire slide to capture more variation. Another explanation for the limited variability in bile duct proliferation may indicate that the development of NAFLD may not be advanced enough to demonstrate sufficient variation among portal triads to achieve statistical significance. In these mink, Pal (2011) reported that mink fasted for 0, 1, and 3 days developed mild fatty liver according to mean NAI scores, while mink fasted for 5 and 7 days had moderate fatty liver. This further supports the idea that a more advanced disease progression may be necessary for any significant changes in bile duct morphology to become apparent. Nagarajan *et al.* (2008) indicate that newly formed bile ductules were associated with fibrosis, which was not present in the liver of the fasted mink in the study (Pal 2011). Future studies should focus on immunostaining enabling a more assured identification of bile ducts in the liver.

CHAPTER 7.0 CONCLUSION

In summary, fasting of mink resulted in an increase in liver mRNA expression of both MCP-1 and TNF-α with the highest expression occurring in mink fasted for 7 and 5 days, respectively. Fasting mink resulted in a significant correlation between TNF-α and MCP-1 liver mRNA expression levels, while TNF-α was also strongly correlated with liver fat percent. An increase in liver inflammation may be explained by the excess mobilization of n-3 PUFA resulting in a pro-inflammatory physiological state and the increase in liver lipids, which is correlated with an increase liver mRNA expression of TNF-α. Re-feeding mink after a period of fasting returned liver mRNA expression levels of TNF-α and MCP-1 back to normal, which highlights the liver's ability to restore homeostasis after a period of re-feeding. Fasting had no significant effect on bile duct quantity; however further research is required to determine whether a fatty liver disease model with developed fibrosis would give a different result. In conclusion, this project has identified two important biomarkers involved in the development of fatty liver in mink, namely TNF-α and MCP-1. It is anticipated that future research will focus on the development of *in vivo* testing for these inflammatory markers enabling early detection of fatty liver in mink.

REFERENCES

Adams LA, Angulo P, and Lindor KD. Nonalcoholic fatty liver disease. CMAJ 2005; 172:899-905.

Aggarwal BB. Signaling pathways of the TNF superfamily: a double-edged sword. Nat 2003; 3:745-756.

Antuna-Puente B, Feve B, Fellahi S, and Bastard JP. Adipokines: The missing link between insulin resistance and obesity. Diabetes Metab 2008; 34:2-11.

Baeck C, Wehr A, Karlmark KR, Heymann F, Vucur M, Gassler N, Huss S, Klussmann S, Eulberg D, Luedde T, Trautwein C, and Tacke F. Pharmacological inhibition of the chemokine CCL2 (MCP-1) diminishes liver macrophage infiltration and steatohepatitis in chronic hepatic injury. Gut 2012; 61:416-426.

Baffy G. Kupffer cells in non-alcoholic fatty liver disease: The emerging view. J Hepatol 2009; 51:212-223.

Baratta, JL, Ngo A, Lopez B, Kasabwalla N, Longmuir KJ, and Robertson RT. Cellular organization of normal mouse liver: A histological, quantitative immunocytochemical, and fine structural analysis. Histochem Cell Biol 2009; 131:713-726.

Bautista AP. The role of Kupffer cells and reactive oxygen species during acute and chronic ethanol intoxication. Alcohol Clin Exp Res 1998; 22:255–259.

Bedogni G, Miglioli L, Masutti F, Tiribelli C, Marchesini G, and Bellentani S. Prevalence of and risk factors for nonalcoholic fatty liver disease: the Dionysus nutrition and liver study. Hepatol 2005; 42:44-52.

Bellentani S, Scaglioni S, Marino M, and Bedogni G. Epidemiology of non-alcoholic fatty liver disease. Dig Dis 2010; 28:155–161.

Bertola A, Bonnafous S, Anty R, Patouraux S, Saint-Paul MC, Iannelli A, Gugenheim J, Barr J, Mato JM, Le Marchand-Brustel, Tran A, and Gual P. Hepatic expression patterns of inflammatory and immune response genes associated with obesity and NASH in morbidly obese patients. PLoS ONE 2010; 5:e13577.

Bilzer M, Roggel F, and Gerbes AL. Role of Kupffer cells in host defense and liver disease. Liver Int 2006; 26:1175-1186.

Biourge VC, Groff JM, Munn RJ, Kirk CA, Nyland TG, Madeiros VA, Morris JG, and Rogers QR. Experimental induction of hepatic lipidosis in cats. Am J Vet Res 1994; 55:1291-1302.

Bjornvad CR, Elnif J, and Sangild PT. Short-term fasting induces intra-hepatic lipid accumulation and decreases intestinal mass without reduced brush-border enzyme activity in mink (*Mustela vison*) small intestine. J Comp Physiol 2004; 174:625–632.

Blanchard G, Paragon BM, Sérougne C, Férézou J, Milliat F, and Lutton C. Plasma lipids, lipoprotein composition and profile during induction and treatment of hepatic lipidosis in cats and the metabolic effect of one daily meal in healthy cats. J Anim Physiol Anim Nutr 2004; 88:73–87.

Browning JD, Szczepaniak LS, Dobbins R, Nuremberg P, Horton JD, Cohen JC, Grundy SM, and Hobbs HH. Prevalence of hepatic steatosis in an urban population in the United States: impact of ethnicity. Hepatol 2004; 40:1387-1395.

Brunt EM. Nonalcoholic steatohepatitis. Sem Liver Disease 2004; 24:1-20.

Brunt EM. Nonalcoholic steatohepatitis: pathologic features and differential diagnosis. Semin Diagn Pathol 2005; 22:330-339.

Brunt EM, Kleiner DE, Wilson LA, Unalp A, Behling CE, Lavine JE, and Neuschwander-Tetri BA. Portal chronic inflammation in nonalcoholic fatty liver disease a histologic marker of advanced NAFLD clinicopathologic correlations from the NASH clinical research network. Hepatol 2009; 49:809-820.

Brunt EM, Janney CG, Di Bisceglie AM, Neuschwander-Tetri BA, and Bacon BR. Nonalcoholic steatohepatitis: a proposal for grading and staging the histological lesions. Am J Gastroenterol 1999; 94: 2467-2474.

Capurso C, and Capurso A. From excess adiposity to insulin resistance: The role of free fatty acids. Vascular Pharmacol 2012; 57:91-97.

Caballero T, Gila A, Sánchez-Salgado G, Muñoz de Ruedaz P, León J, Delgado S, Muñoz JA, Caba-Molina M, Carazo A, Ruiz-Extremera A, and Salmerón J. Histological and immunohistochemical assessment of liver biopsies in morbidly obese patients. Histol Histopathol 2012; 27:459-466.

Chalasani N, Wilson L, Kleiner DE, Cummings OW, Brunt EM, and Unalp A. Relationship of steatosis grade and zonal location to histological features of steatohepatitis in adults patients with non-alcoholic fatty liver disease. J Hepatol 2008; 48:829-834.

Chen X, Xun K, Chen L, and Wang Y. TNF-α, a potent lipid metabolism regulator. Cell Biochem Funct 2009; 27:407–416.

Chiba M, Sasaki M, Kitamura S, Ikeda H, Sato Y, and Nakanuma Y. Participation of bile ductular cells in the pathological progression of non-alcoholic fatty liver disease. J Clin Pathol 2011; 64:564-570.

Clària J, González-Périz, López-Vicario C, Rius B, and Titos E. New insights into the role of macrophages in adipose tissue inflammation and fatty liver disease: modulation by endogenous omega-3 fatty acid-derived lipid mediators. Front Immunol 2011; 49:1-8.

Clausen TN, Olesen CR, Hansen O, and Wamberg S. Nursing sickness in lactating mink (*Mustela vison*) I. Epidemiological and pathological observations. Can J Vet Res 1992; 56:89-94.

Coppack SW. Pro-inflammatory cytokines and adipose tissue. Proc Nutr Soc 2001; 60:349-356.

Czaja MJ, Geerts A, Xu J, Schmiedeberg, and Y Ju. Monocyte chemoattractant protein 1 (MCP-1) expression occurs in toxic rat liver injury and human liver disease. J Leukocyte Biol 1994; 55:120-126.

Day CP. From fat to inflammation. Gastroenterol 2006; 130:207-210.

de Alwis NM, and Day CP. Non-alcoholic fatty liver disease: the mist gradually clears. J Hepatol 2008; 48:S104–S112.

Degré D, Lemmers A, Gustot T, Ouziel R, Trépo E, Demetter P, Verset L, Quertinmont E, Vercruysse V, Le Moine O, Devière J, and Moreno C. Hepatic expression of CCL2 in alcoholic liver disease is associated with disease severity and neutrophil infiltrates. Clin Exp Immunol 2012; 169:302-310.

Demetris AJ, Seaberg EC, Wennerberg TA, and Michalopoulos G. Ductular reaction after submassive necrosis in humans. Special emphasis on analysis of ductular hepatocytes. Am J Pathol 1996; 149:439-448.

Diethl AM. TNF-alpha is not the cause of fatty liver disease in obese diabetic mice. Nat Med 2001; 7:2-3.

Dowman JK, Tomlinson JW, and Newsome PN. Pathogenesis of non-alcoholic fatty liver disease. Q J Med 2010; 103:71-83.

Elias JA, and Lentz V. IL-1 and tumor necrosis factor synergistically stimulate fibroblast IL-6 production and stabilize IL-6 mRNA. J Immunol 1990; 145:161-166.

Endo M, Masaki T, Seike M, and Yoshimatsu H. TNF-α induces hepatic steatosis in mice by enhancing gene expression of sterol regulatory element binding protein-1c (SREBP-1c). Exp Biol and Med 2007; 232:614-621.

Enomoto K, Nishikawa Y, Omori Y, Tokairin T, Yoshida M, Ohi N, Nishimura T, Yamamoto Y, and Qinchang L. Cell biology and pathology of liver sinusoidal endothelial cells. Med Electr Microsc 2004; 37:208-215.

Essani NA, Mcguire GM, Manning AM, and Jaeschke H. Differential induction of mRNA for ICAM-1 and selectins in hepatocytes, Kupffer cells, and endothelial cells during endotoxemia. Biochem Bioph Res Comm 1995; 211:74-82.

Evans WH, Kremmmer T, and Culvenor JG. Comparison of the composition of bile and a liver bile-canalicular plasma-membrane subfraction. Biochem J 1976; 154:589-595.

Fabbrini E, Sullivan S, and Klein S. Obesity and nonalcoholic fatty liver disease: biochemical, metabolic, and clinical implications. Hepatol 2010; 51:679-689.

Farrell GC, and Larter CZ. Non-alcoholic fatty liver disease: from steatosis to cirrhosis. Hepatol 2006; 43:S99-S112.

Feingold KR, Serio MK, Adi S, and Moser AH, and Grunfeld C. Tumor necrosis factor stimulates hepatic lipid synthesis and secretion. Endocrinol 1989; 124:2336–2342.

Feldstein AE, Werneburg NW, Canbay A, Guicciardi ME, Bronk SF, and Rydzewski R. Free fatty acids promote hepatic lipotoxicity by stimulating TNF-alpha expression via a lysosomal pathway. Hepatol 2004; 4:185-194.

Gabay C. Interleukin-6 and chronic inflammation. Arthritis Res Ther 2006; 8:S3.

Gormaz JG, Rodrigo R, Videla LA, and Beems M. Biosynthesis and bioavailability of long-chain polyunsaturated fatty acids in non-alcoholic fatty liver disease. Prog Lipid Res 2010; 49:407-419.

Griffin B. Feline hepatic lipidosis: pathophysiology, clinical signs, and diagnosis. Compendium 2000; 22: 847-858.

Hall, TA. BioEdit: a user-friendly biological sequence alignment editor and analysis program for Windows 95/98/NT. Nucl Acids Symp Ser 1999; 41:95-98.

Hamaguchi M, Takeda N, Kojima T, Ohbora A, Kato T, Sarui H, Fukui M, Nagata C, and Takeda J. Identification of individuals with non-alcoholic fatty liver disease by the diagnostic criteria for the metabolic syndrome. World J Gastroenterol 2012; 18:1508–1516.

Haukeland JN, Damas JK, Konopski Z, Løberg EM, Haahand T, Goverud I, Torjesen PA, Birkeland K, Bjøro K, and Ankrust P. Systemic inflammation in non-alcoholic fatty liver disease is characterized by elevated levels of CCL2. J Hepatol 2006; 44:1167-1174.

Haüssinger D. Nitrogen metabolism in liver: structural and functional organization and physiological relevance. Biochem J 1990; 267:281-290.

Heinrich PC, Castell JV, and Andus T. Interleukin-6 and the acute phase response. Biochem 1990; 265:621-636.

Hotamisligil GS, Arner P, Caro JF, Atkinson RL, and Spiegelman BM. Increased adipose tissue expression of tumor necrosis factor alpha in human obesity and insulin resistance. J Clin Invest 1995; 95:2409-2415.

Hunter BD, and Lemieux N. Mink: Biology, health and disease. Guelph, Ont. Graphic and print services: University of Guelph. 1996.

Iimuro Y, Gallucci RM, Luster MI, Kono H, and Thurman RG. Antibodies to tumor necrosis factor alpha attenuate hepatic necrosis and inflammation caused by chronic exposure to ethanol in the rat. Hepatol 1997; 6:1530-1537.

Imamura M, Ogawa T, Sasaguri Y, Chayama K, and Ueno H. Suppression of macrophage infiltration inhibits activation of hepatic stellate cells and liver fibrogenesis in rats. Gastroenterol 2005; 128:138-146.

Isakson P, Hammarstedt A, Gustafson B, and Smith U. Impaired preadipocyte differentiation in human abdominal obesity role of wnt, tumor necrosis factor-alpha, and inflammation. Diabetes 2009; 58:1550-1557.

Kassel KM, Guo GL, Tawfik O, and Luyendyk JP. Monocyte chemoattractant protein-1-deficiency does not affect steatosis or inflammation in livers of mice fed a methionine-choline-deficient diet. Lab Invest 2010; 90:1794–1804.

Katz S, Pillarisetty VG, Bleier JI, Shah AB, and DeMatteo RP. Liver sinusoidal endothelial cells are insufficient to activate T cells. J Immunol 2004; 173:230-235.

Kersten S, Seydoux J, Peters JM, Gonzalez FJ, Desvergne B, and Wahli W. Peroxisome proliferator-activated receptor α mediates the adaptive response to fasting. J Clin Invest 1999; 103:1489-1498.

Kibbe WA. 'OligoCalc: an online oligonucleotide properties calculator'. Nucleic Acids Res 2007; 35(webserver issue): May 25.

Kindt TJ, Goldsby RA, and Osborne BA. Kuby Immunology. New York, NY: W.H Freedman and Company; 2007.

Kisseleva T, and Brenner DA. Role of hepatic stellate cells in fibrogenesis and the reversal of fibrosis. J Gasteroenterol Hepatol 2007; 22:S73-S78.

Kleiner DE, Brunt EM, Van Natta M, Behling C, Contos MJ, Cummings OW, Ferrell LD, Liu Y-C, Torbenson MS, Unalp-Arida A, Yeh M, McCullough AJ, and Sanyal AJ. Design and validation of a histological scoring system for nonalcoholic fatty liver disease. Hepatology 2005; 41:1313–1321.

Korhonen H, and Niemelä P. Effect of feeding level during autumn and winter on breeding weight and result in single and pair-housed minks. Agric Food Sci Finl 1997; 6:305-312.

Kotronen T, Westerbacka J, Bergholm R, Pietiläinen KH. and Yki-Järvinen H. Liver fat in the metabolic syndrome. J Clin Endocrinol Metab 2007; 92:3490-3497.

Lee H, Shi W, Tontonoz P, Wang S, Subbanagounder G, Hedrick CC, Hama S, Borromeo C, Evans RM, Berliner JA, and Nagy L. Role for peroxisome proliferator-activated receptor alpha in oxidized phospholipid-induced synthesis of monocyte chemotactic protein-1 and interleukin-8 by endothelial cells. Circ Res 2000; 87:516–521.

Leevy CM, Thompson A, and Baker H. Vitamins and liver injury. Am J Clin Nutr 1970; 4:493-499.

Li ZZ, Berk M, McIntyre TM, and Feldstein AF. Hepatic lipid partitioning and liver damage in nonalcoholic fatty liver disease: role of stearoyl-CoA desaturase. J Biol Chem 2009; 284:5637-5644.

Lin HZ, Yang SQ, Chuckaree C, Kuhajda F, Ronnet G, and Diehl AM. Metformin reverses fatty liver disease in obese, leptin-deficient mice. Nat Med 2000; 9:998-1003.

Lin HZ, Yang SQ, Zeldin G, and Diehl AM. Chronic ethanol consumption induces the production of tumor necrosis factor-alpha and related cytokines in liver and adipose tissue. Alcohol Clin Exp Res 1998; 22:231S-237S.

Liquori GE, Calamita G, Cascella D, Mastrodonato M, Portincasa P, and Ferri D. An innovative methodology for the automated morphometirc and quantitative estimation of liver steatosis. Histol Histopathol 2009; 24:49-60.

Lisowski P, Pierzchala M, Goscik J, Pareek CS, and Zwierzchowski L. Evaluation of reference genes for studies of gene expression in the bovine liver, kidney, pituitary, and thyroid. J Appl Genet 2008; 49:367-372.

Luyendyk JP, Sullivan BP, Guo GL, and Wang R. Tissue factor deficiency and protease activated receptor-1 deficiency reduce inflammation elicited by diet-induced steatohepatitis in mice. Am J Pathol. 2010; 176:177–186.

Maher JJ. Cytokines: overview. Semin Liver Dis 1999; 19:109–115.

Mantovani A, Sica A, Sozzani S, Allavena P, Vecchi A, and Locati M. The chemokine system in diverse forms of macrophage activation and polarization. Trends Immunol 2004; 25:677–686.

Marion AW, Baker AJ, and Dhawan A. Fatty liver disease in children. Arch Dis Child 2004; 89:648-652.

Marra F, DeFranco R, Grappone C, Milani S, Pastacaldi S, Pinzani M, Romanelli RG, Laffi G, and Gentilini P. Increased expression of monocyte chemotactic protein-1 during active hepatic fibrogenesis. Am J Pathol 1998; 152:423-430.

Marra F, Valente AJ, Pinzani M, and Abboud HE. Cultured human liver fat storing cells produce monocyte chemotactic protein-1. Regulation for proinflammatory proteins. J Clin Invest 1993; 92:1674-1680.

Matteoni CA, Younossi ZM, Gramlich T, Boparai N, Liu YC, and McCullough AJ. Nonalcoholic fatty liver disease: a spectrum of clinical and pathological severity. Gastroenterol 1999: 116:1413-1419.

Merat S, Khadem-Sameni F, Nouraie M, Derakhshan M, Mohammad Tavangar S, Mossaffa S, Malekzadeh R, and Sotoudeh M. A modification of the Brunt system for scoring liver histology of patients with non-alcoholic fatty liver disease. Arch Iran Med 2010; 13:38-44.

Mofrad PS, and Sanyal AJ. Nonalcoholic fatty liver disease. Medscape Gen Med 2003; 5:1-8.

Murao K, Ohyama T, Imachi H, Ishida T, Min Cao W, Namihira H, Sato M, Wong NCW, and Takahara J. TNF-α stimulation of MCP-1 expression is mediated by the akt/pkb signal transduction pathway in vascular endothelial cells. Biochem Biophysical Res Comm 2000; 276:791-796.

Mustonen AM, Käkelä R, Käkelä A, Pyykönen T, Aho J, and Nieminen P. Lipid metabolism in the adipose tissues of a carnivore, the raccoon dog, during prolonged fasting. Exp Biol Med 2007; 232:1095-1107.

Mustonen AM, Puukka M, Rouvinen-Watt K, Aho J, Asikainen J, Nieminen P. Response to fasting in an unnaturally obese carnivore, the captive European polecat *Mustela putorius*. Exp Biol Med 2009; 234:1287-1295.

Mustonen AM, Pyykönen T, Paakkonen T, Ryökkynen A, Asikainen J, Aho J, Mononen J, and Nieminen P. Adaptations to fasting in the American mink (*Mustela vison*): carbohydrate and lipid metabolism. Comp Biochem Physiol 2005; 140:195-202.

Nagarajan P, Venkatesan R, Kumar M, Usmani A, and Majumdar SS. *Macaca radiata* (bonnet monkey): a spontaneous model of nonalcoholic fatty liver disease. Liver Int 2008; 5:856-864.

Nagelkerke JF, Barto KP, and Van Berkel JC. *In vivo* and *in vitro* uptake and degradation of acetylated low density lipoprotein by rat liver endothelial, Kupffer, and parenchymal cells. J Biological Chem 1983; 20:12221-12227.

Nanji AA, Jokelainen K, Fotouhinia M, Rahemtulla A, Thomas P, Tipoe GL, Su GL, and Dannenberg AJ. Increased severity of alcoholic liver injury in female rats: role of oxidative stress, endotoxin, and chemokines. Am J Physiol Gastointest Liver Physiol 2001; 281:G1348-G1356.

Neyrinck AM, Cani PD, Dewulf EM, De Backer F, Bindels LB, and Delzenne NM. Critical role of Kupffer cells in the management of diet-induced diabetes and obesity. Biochem Bioph Res Comm 2009; 385:351-356.

Nicoll RG, Jackson MV, Knipp SS, Zagzebski JA, Steinberg H, and O'Brien RT. Quantitative ultrasonography of the liver in cats during obesity induction and dietary restriction. Res Vet Sci 1998; 64:1-6.

Nieminen P, Käkelä R, Pyykönen T, and Mustonen AM. Selective fatty acid mobilization in the American mink (*Mustela vison*) during food deprivation. Comp Biochem Physiol 2006; 145:81-93.

Nieminen P, Käkelä R, Mustonen AM, Hyvärinen H, and Asikainen J. Exogenous melatonin affects lipids and enzyme activities in mink *(Mustela vison*) liver. Comp Biochem Physiol Part C 2001; 128:201-211.

Nieminen P, Mustonen AM, Kärjä V, Asikainen J, and Rouvinen-Watt K. Fatty acid composition and development of hepatic lipidosis during food deprivation mustelids as a potential animal model for liver steatosis. Exp Biol Med 2009; 234:278-286.

Obstfeld AE, Sugaru E, Thearle M, Francisco AM, Gayet C, Ginsberg HN, Ables EV, and Ferrante Jr AW**.** C-C chemokine receptor 2 (CCR2) regulates the hepatic recruitment of myeloid cells that promote obesity-induced hepatic steatosis. Diabetes 2010; 59:916–925.

Odegaard JI, and Chawla A. Mechanisms of macrophage activation in obesity-induced insulin resistance. Nat Clin Pract Endocrinol Metab 2008; 11:619-626.

O'Shea JJ, and Murray PJ. Cytokine signaling modules in inflammatory responses. Immun 2008; 28:477-487.

Pal C. Detection of endoplasmic reticulum stress and progression of steatohepatitis in mink (*Neovison vison*) with fatty liver. M.Sc. thesis, 2011. Dalhousie University, Halifax, Canada.

Palou M, Priego T, Sánchez J, Villegas E, Rodríguez AM, and Picó C. Sequential changes in the expression of genes involved in lipid metabolism in adipose tissue and liver in response to fasting. Eur J Physiol 2008; 456:825-836.

Persson S, Bäcklin BM, Kindahl H, Brunström B, and Magnusson U. Influence of age, nutritional status, and season on the reproductive system in wild male mink (*Neovison vison*). Eur J Wildl Res 2011; 57:1057-1063.

Pietiläinen KH, Rissanen A, Kaprio J, Mäkimattila S, Häkkinen AM, Westerbacka J, Sutinen J, Vehkavaara S, and Yki-Järvinen H. Acquired obesity is associated with increased liver fat, intra-abdominal fat, and insulin resistance in young adult monozygotic twins. Am J Physiol Endocrinol Metab 2005; 288:E768-E774.

Popa C, Netea MG, van Riel PLCM, van der Meer JWM, and Stalenhoef AFH. The role of TNF-α in chronic inflammatory conditions, intermediary metabolism, and cardiovascular risk. J Lipid Res 2007; 48:751-762.

Qin B, Anderson R, and Adeli K. Tumor necrosis factor-α directly stimulates the overproduction of hepatic apolipoprotein B100-containing VLDL via impairment of hepatic insulin signaling. Am J Physiol Gastrointest Liver Physiol 2008; 294:G1120–G1129.

Rakha EA, Adamson L, Bell E, Neal K, Ryder SD, Kaye PV, and Aithal G. Portal inflammation is associated with advanced histological changes in alcoholic and non-alcoholic fatty liver disease. J Clin Pathol 2010; 63:790-795.

Ramaiah SK, and Jaeschke H. Role of neutrophils in the pathogenesis of acute inflammatory liver injury. Toxicol Pathol 2007; 35:757-766.

Rappaport AM, MacPhee PJ, Fisher MM, and Philips MJ. The scarring of the liver acini (cirrhosis) tridimensional and microcirculatory considerations. Pathol Anat J 1983; 402:107-137.

Renier G, Clement I, Desfaits AC, and Lambert A. Direct stimulatory effect of insulin-like growth factor-1 on monocyte and macrophage tumor necrosis factor-alpha production. Endcrinol 1996; 137:4611-4618.

Ross M, and Pawlina W. Digestive system III: Liver, Gallbladder, and Pancreas. In: Histology a Text and Atlas with Correlated Cell and Molecular Biology. Baltimore, MD: Lippincott Williams & Wilkins; 2006:576-602.

Rouvinen-Watt K. Nursing sickness in the mink a metabolic mystery or a familiar foe? Can J Vet Res 2003; 67:161-168.

Rouvinen-Watt K, Harris L, Dick M, Pal C, Lei S, Mustonen AM, and Nieminen P. Role of hepatic *de novo* lipogenesis in the development of fasting-induced fatty liver in the American mink (*Neovison vison*). British J Nutr 2012; 108: 1360-1370.

Rouvinen-Watt K, and Hynes AM. Mink nursing sickness survey in North America. Scientifur 2004; 28: 71-78.

Rouvinen-Watt K, Mustonen AM, Conway R, Pal C, Harris L, Saarela S, Strandberg U, and Nieminen P. Rapid development of fasting-induced hepatic lipidosis in the American mink (*Neovison vison*): effects of food deprivation and re-alimentation on body fat depots, tissue fatty acid profiles, hematology and endocrinology. Lipids 2010; 45:111-128.

Rozen S and Skaletsky HJ. 2000. Primer3 on the WWW for general users and for biologist programmers. In: Krawetz S, Misener S (eds) Bioinformatics Methods and Protocols: Methods in Molecular Biology. Humana Press, Totowa, NJ, pp 365-386.

Rull A, Rodríguez F, Aragonès G, Marsillach J, Beltrán R, Alonso-Villaverde C, Camps J, and Joven J. Hepatic monocyte chemoattractant protein-1 is upregulated by dietary cholesterol and contributes to liver steatosis. Cytokine 2009; 48:273–279.

Rydell-Törmänen K, Uller L, and Erjefält JS. Neutrophil cannibalism: a back up when the macrophage clearance system is insufficient. Resp Res 2006; 7:143-150.

Sasaki M, Ikeda H, and Yamaguchi J. Bile ductular cells undergoing cellular senescence increase in chronic liver diseases along with fibrous progression. Am J Clin Pathol 2010; 133:212-223.

Savage DB, Petersen KF, and Shulman GI. Disordered lipid metabolism and the pathogenesis of insulin resistance. Physiol Rev 2007; 87:507–520.

Schneider RR, and Hunter DB. Nursing sickness in Mink: Clinical and post-mortem findings. Vet Pathol 1993; 30:512-521.

Schwimmer JB, Deutsch R, Kahen T, Lavine JE, Stanley C, and Behling C. Prevelance of fatty liver in children and adolescents. Pediatrics 2006; 118:1388-1393.

Seimiya Y, Kikuchi F, Tanaka S, and Ohshima K. Pathological observations of nursing sickness in mink. Jpn J Vet Sci 1988; 50:255-257.

Sellaro TL. Maintenance of primary human hepatocyte function *in vitro* by extracellular matrix scaffolds. Proquest Dissertations and Theses 2008; 307:178-185.

Senoo H. Structure and function of hepatic stellate cells. Med Electr Microsc 2004; 37:3-15.

Seth D, Haber PS, Syn WK, Diehl AM, and Day CP. Pathogenesis of alcohol-induced liver disease: Classical concepts and recent advances. J Gastroentrol Hepatol 2011; 26:1089-1105.

Smedsrød B, Pertoft H, Gustafson S, and Laurent TC. Scavenger functions of the liver endothelial cell. Biochem J 1990; 266:313-327.

Smith DG, and Schenk MP. Mink Dissection Atlas. Englewood, Colorado: Morton publishing company; 1999.

Smith U, Andersson CX, Gustafson B, Hammarstedt A, Isakson P, and Wallerstedt E. Adipokines, systemic inflammation and inflamed adipose tissue in obesity and insulin resistance. Int Cong Ser 2007: 1303:31-34.

Straus DS, and Takemoto CD. Effect of fasting on insulin-like growth factor-I (IGF-1) and growth hormone receptor mRNA levels and IGF-1 gene transcription in rat liver. Mol Endo 1990; 4:91-100.

Tamura Y, Sugimoto M, Murayama T, Ueda Y, Kanamori H, Ono K, Ariyasu H, Akamizu T, Kita T, Yokode M, and Aria Y. Inhibition of CCR2 ameliorates insulin resistance and hepatic steatosis in db/db mice. Arterioscler Thromb Vasc Biol 2008; 28:2195–2201.

Tessari P, Coracina A, Cosma A, and Tiengo A. Hepatic lipid metabolism and non-alcoholic fatty liver disease. Nutr Metab Cardiovasc Dis 2009; 19:291-302.

Tous M, Ferré N, Rull A, Marsillach J, Coll B, Alonso-Villaverde C, Camps J, and Joven J. Dietary cholesterol and differential monocyte chemoattractant protein-1 gene expression in aorta and liver of apo E-deficient mice. Biochem Biophys Res Commun. 2006; 340:1078–1084.

Trauner M, Arrese M, and Wagner M. Fatty liver and lipotoxicity. Biochim Biophys Acta 2010; 1801:299–310.

Trayhurn P, and Wood I. Signaling role of adipose tissue: adipokines and inflammation in obesity. Biochem Soc Trans 2005; 33:1078-1081.

Vissers MCM, and Hampton MB. The role of oxidants and vitamin C on neutrophil apoptosis and clearance. Biochem Soc Trans 2004; 32:499-501.

Vuppalanchi R, and Chalasani N. Nonalcoholic fatty liver disease and nonalcoholic steatohepatitis: selected practical issues in their evaluation and management. Hepatol 2009; 49:306–317.

Weisberg SP, Hunter D, Huber R, Lemieux J, Slaymaker S, Vaddi K, Charo I, Leibel RL, and Ferrante Jr. AW. CCR2 modulates inflammatory and metabolic effects of high-fat feeding. J Clin Invest 2006; 116:115-124.

Westerbacka J, Lammi K, Häkkinen AM, Rissanen A, Salminen I, Aro A, and Yki-Järvinen H. Dietary fat content modifies liver fat in overweight nondiabetic subjects. J Endocrinol Metab 2005; 90:2804-2809.

Westerbacka J, Kolak M, Kiviluoto T, Arkkila P, Sirén J, Hamsten A, Fisher RM, and Yki-Järvinen H. Genes involved in fatty acid partitioning and binding, lipolysis, monocyte/macrophage recruitment, and inflammation are overexpressed in the human fatty liver of insulin-resistant subjects. Diabetes 2007; 56:2759-2765.

Wormald S, and Hilton DJ. Inhibitors of cytokine signaling transduction. J Biol Chem 2004; 279:821-824.

Yang J, Park Y, Zhang H, Gao X, Wilson E, ZimmerW, Abbott L, and Zhang C. Role of MCP-1 in tumor necrosis factor-α-induced endothelial dysfunction in type 2 diabetic mice. Am J Physiol Heart Circ Physiol 2009; 297:H1208-H1216.

Yerian L. Histopathological evaluation of fatty and alcoholic liver diseases. J Digest Dis 2011; 12: 17-24.

Yin M, Wheeler MD, Kono H, Bradford BU, Gallucci RM, Luster MI, and Thurman RG. Essential role of tumor necrosis factor α in alcohol-induced liver injury in mice. Gastroenterol 1999; 117:942-952.

Yoshida H, Takamura N, Shuto T, Ogata K, Tokunaga J, Kawai K, and Kai H. The citrus flavonoids hesperetin and naringenin block the lipolytic actions of TNF-α in mouse adipocytes. Biochem Biophys Res Comm 2010; 394:728–732.

Xu L, Ma X, Cui B, Li X, Ning G, and Wang S. Selection of reference genes for qRT-PCR in high fat diet-induced hepatic steatosis mice model. Mol Biotechnol 2011; 48: 255-262.